8-2012

Outcrop Investigation of the Reeds Spring (Boone, Mississippian) of the Hindsville Quarry using Terrestrial Lidar

Terryl Glenn Daniels
University of Arkansas, Fayetteville

OUTCROP INVESTIGATION OF THE REEDS SPRING (BOONE, MISSISSIPPIAN) OF THE HINDSVILLE QUARRY USING TERRESTRIAL LIDAR

OUTCROP INVESTIGATION OF THE REEDS SPRING (BOONE, MISSISSIPPIAN) OF THE HINDSVILLE QUARRY USING TERRESTRIAL LIDAR

A Thesis Submitted in Partial fulfillment
of the requirements for the degree of
Master of Science in Geology

By

Terryl G. Daniels Jr.
The Pennsylvania State University
Bachelor of Science in Geosciences, 2009

August 2012
University of Arkansas

ABSTRACT

In northern Oklahoma and southern Kansas the Reeds Springs Formation (Boone, Mississippian) is a hydrocarbon exploration objective (Mazullo et al, 2011). The Hindsville quarry located in the northeastern portion of Washington County in Arkansas is the focus of this study. The objective of this study is to characterize the Reeds Spring at the Hindsville Quarry. The use of terrestrial light detecting and ranging(LiDAR) is used to assist in the characterization of the quarry.

The unit architecture within the Hindsville Quarry outlines varying transitional periods that give insight into the deposition of the Reeds Springs Formation. There are comparable formations within the Carboniferous that serve as helpful analogues in explaining the complexities seen in the Hindsville Quarry. Diffusive process (turbidity currents or debris flows) and physical energy flux (winds, waves, and storms) played a large part in defining the sedimentary structures found within the Hindsville Quarry. These mechanisms in depositional process demonstrate that the use of sub aerial exposures are not needed to explain erosive surfaces.

Terrestrial LiDAR is used to identify stratigraphic pattern, bedding planes, and determine the orientation of inaccessible quarry walls. The effects of distance and incidence angle, resolution of the scan, and the ability to discriminate varying lithologies played a role in the assessment of the geologic outcrops. The surveyed dataset allowed detail measurement to be accomplished. The non-contact techniques of investigating geologic outcrops through Terrestrial LiDAR cannot replace transitional methods of geologic investigation, but complement it.

This thesis is approved for recommendation
to the Graduate Council.

Thesis Director:

____
Dr. Doy L. Zachry

Thesis Committee:

____
Dr. Jackson Cothren

____
Dr. Xiangyang Xie

THESIS DUPLICATION RELEASE

I hereby authorize the University of Arkansas Libraries to duplicate this Thesis when needed for research and/or scholarship

Agreed ____
Terryl Glenn Daniels Jr.

Refused ____
Terryl Glenn Daniels Jr.

ACKNOWLEDGMENTS

I would like to first thank my advisor, Dr. Doy L Zahry for adjustments, insights, and encouragement throughout the thesis process. Dr. Jack Cothren for support and guidance. Dr. Xiangyang Xie for his reviews during the editorial process. The particularly guiding discussions of Dr. Walter Manger and Dr. J. Van Brahana has helped to shape my research goals and refine my analysis of the Boone Formation.

There are many people who have helped with data collection or analysis of this work. Malcolm Williamson for his assistance with Terrestrial LiDAR. Taylor Friesenhahn for many discussions and his assistance. Caitlin Stevens for her assistance in Cyclone. Katy Kniernm and Byron Winston for their insight. I would like to thank the CDEP program for allowing me to reach this point in my academics.

TABLE OF CONTENTS

LIST OF FIGURES **pg**

Introduction

The understanding of the geometry and facies distribution is an important component in the evaluation of a hydrocarbon reservoir. In Kansas and Oklahoma the Reeds Spring Formation is growing in interest for hydrocarbon exploration and development. The characterization of Osagean Reeds Spring Formation can lead to further insight into the development of plays within the midcontinent (Mazzullo et al, 2011). Outcrops of Reeds Spring Formations at Beaver Lake (Section 10 T20N-R27W) and Hindsville Quarry (Section 10 T17N-R28W) are the study sites of this research (figure 1). Fundamental information such as fractures, stratigraphic patterns, and chert content at these outcrops contribute to contribute to further identification of reservoir facies in the subsurface. Although the outcrops to subsurface correlations are miles apart, the outcrop serves as a general point of reference for investigating subsurface characterization (Mazzullo et al, 2011). The integration of field work, photography, and Terrestrial Light Detecting and Ranging (LiDAR) allows for the analysis of these quarries.

The formation name Reeds Spring is not recognized in Arkansas and the outcrops are part of the informal lower Boone Formation (Manger et al, 1988;figure 2). The Mississippian lower Boone Formation is a fine-grained limestone with dark anastomosing chert beds and nodules (Manger et al, 1988). The Boone formation conformably overlies the St. Joe Formation, of Mississippian age. The St. Joe is composed of the Bachelor, Compton, Northview, and Pierson Members. The Hindsville Formation to the west and Batesville Formation to the east unconformably overlie the Boone Formation (Shelby, 1986). The presence of chert and low porosity values of the Boone classifies the Reeds Spring as an unconventional reservoir (Davis, 2007).

In this work, the Reeds Spring Formation at two outcrops have been investigated. The stratigraphic framework was expanded to help identify formation characteristics seen in the subsurface by wireline logs. Traditional field work has been incorporated with Terrestrial LiDAR to identify bedding planes, surface boundaries, and stratigraphic patterns. The evaluation of Terrestrial LiDAR and its ability to assist in a geologic investigation is discussed.

Geologic Setting and Depositional Environment

During the late early Mississippian, a tropic sea covered most of southern North America (Gutschick and Sandberg, 1983; figure 3). North America is inferred to be attached to a south-dipping subducting plate (Lillie et al, 1983). The upper plate is interpreted to be an island arc (Grahame et al, 1975). The two plates had converged by the end of Pennsylvanian time (Gutschick and Sandberg, 1983). Deposits of the Boone Formation reflect transported carbonates on a passive margin conditions (Manger, 2012).

The two study sites are located on the northern Arkansas structural platform and Paleozoic rocks generally exhibit a dip less than 1 degree (Chinn and Konig, 1973). Conodonts from the Boone suggest the formation's depositional setting as rapid and uniform during Osagean time (Liner, 1980).

The Boone Formation has been informally divided into an upper and lower Boone based on the chert development and textural form (Shelby, 1986). The lower Boone chert occurs as nodules, discontinuous bands, and anastomosing bodies usually of a dark color (Giles, 1935). The chert content ranges from 35 to 65 percent. Carbonate mudstone and wackstone facies are dominate. The upper Boone contains light digenetic chert dominated by carbonate packstone and grainstone supported lithology (Liner et al, 1980).

The Boone Formation crops out in northwest Arkansas on the southwestern flanks of the Ozark dome (Hundson, 1986). The deposition of lower Mississippian rocks in northwest Arkansas occurred on the southern edge of a broad shallow carbonate platform called the Burlington Shelf (Lane, 1978). The transition to carbonate mudstone and wackstones in the Lower Boone Formation is an indicator of a gradual deepening of a transgressive sea. The upper Boone was deposited into shallower waters than the lower Boone, and the upper Boone deposits represent a High System Tract. The St. Joe-Boone interval represents an unconformity bound regressive-transgressive sequence (Shelby, 1986).

The depositional environment of the Boone Formation ranges from deep quiet waters below wave base to shallow shelf edge (Liner, 1980). Lane (1978) indicates that Boone Formation’s sediments are representative of progradation. Isopach maps of the Boone Formation in Northwest Arkansas by Linear (1980) and Shelby (1986) depict a lobate pattern and thinning toward the south. Based on lithological descriptions of the Boone Formation, it represents clinothem and/or foreslope positions define in Wilson (1975), shelf margin depofacies in Lane and De Keyser (1980), and foreslope and/or shelf margin in Guschick and Sandberg (1983). The depositional setting of the Lower Boone is in deep water due to the mud-supported lithologies and absence of shallow water indicators (e.g. mud cracks, shallow water fauna, extensive burrowing). Although mudstone dominates the lithology for the lower Boone, packstone and grainstone intervals occur within the lower Boone classification (Van Den Heuval, 1979; Shelby, 1986). Carbonate sediments can be derived in multiple transport processes such as, storm waves, turbidity currents, debris flow, sliding, submarine fans, or even depositional lobes (Boggs, 2006). In carbonate setting re-sedimentation by way of turbidity current may occur as frequent as 1 per 20,000 to 100,000 years (Dorrik et al, 1985). Sedimentary structures formed in cherty

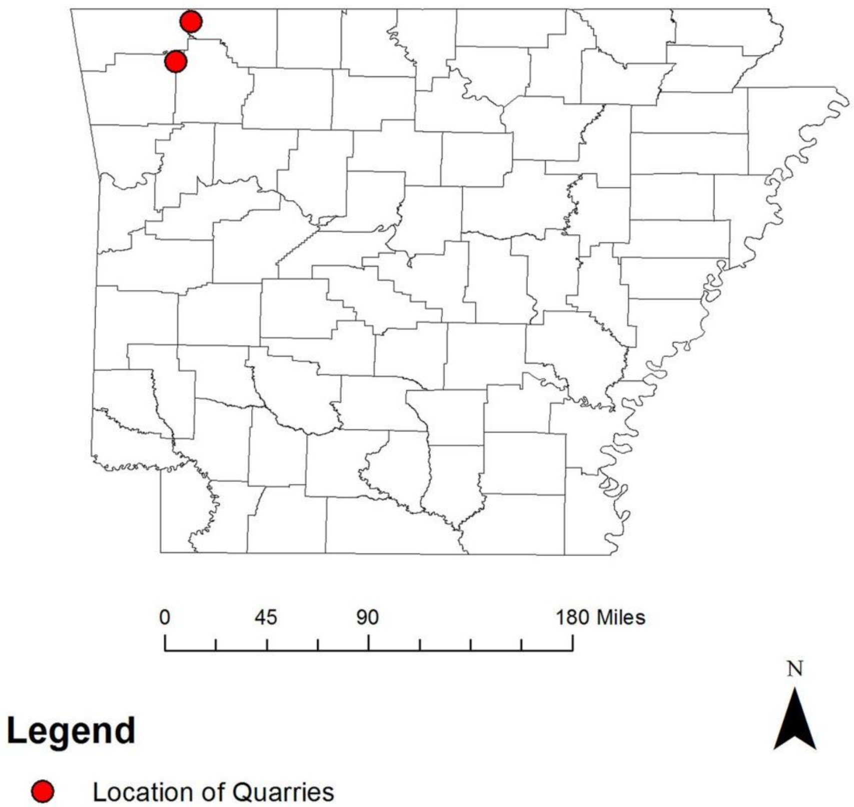

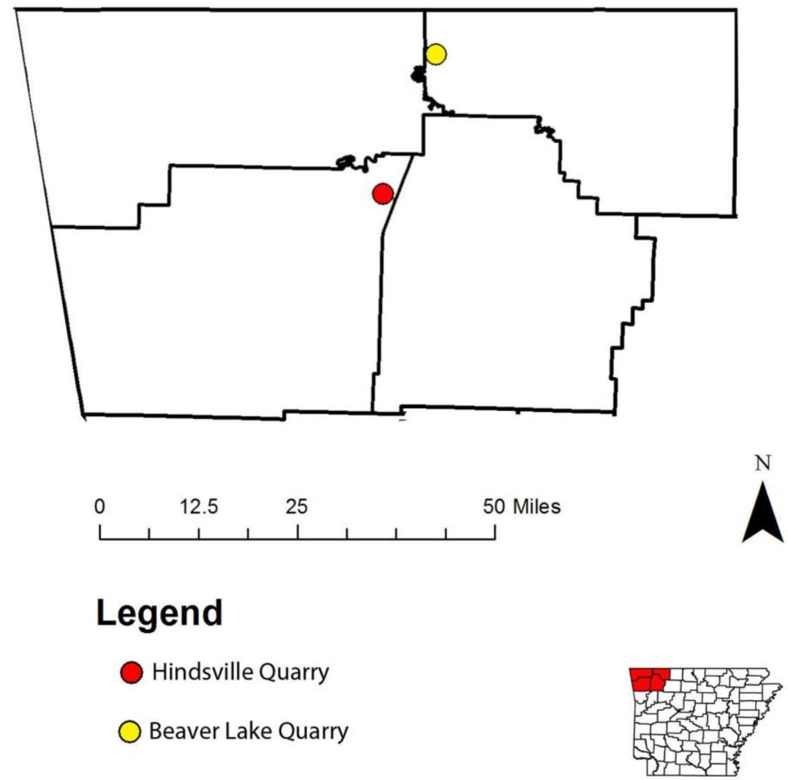

Figure 1. Location of Quarries in Arkansas
The two quarries are located in the northwestern portion of Arkansas. The physiographic region is known as the Ozark Plateau. Within the subset of the Ozark Plateau the quarries are located on the Springfield Plateau. At both of the localities the Boone Formation is exposed.

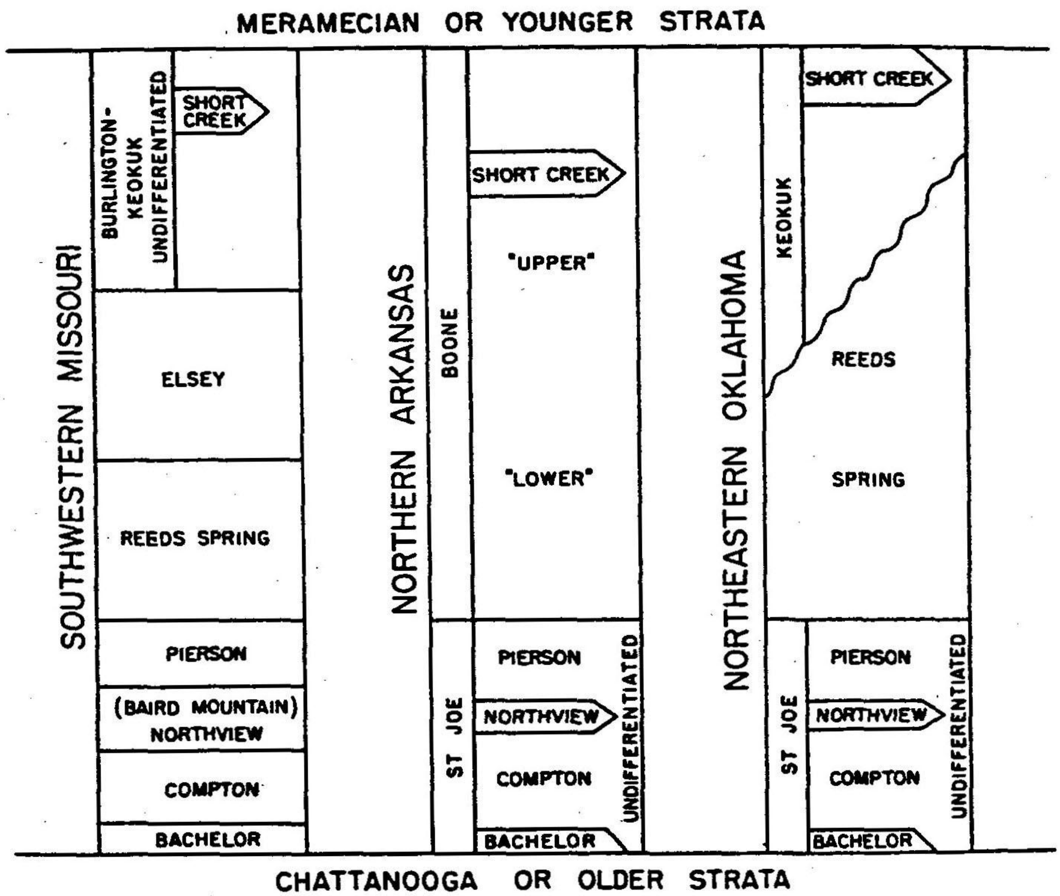

Figure 2. Stratigraphic nomenclature from manger
The tri-state areas nomenclature for the lower Mississippian carbonates. The figure is borrowed from Manger (1988).

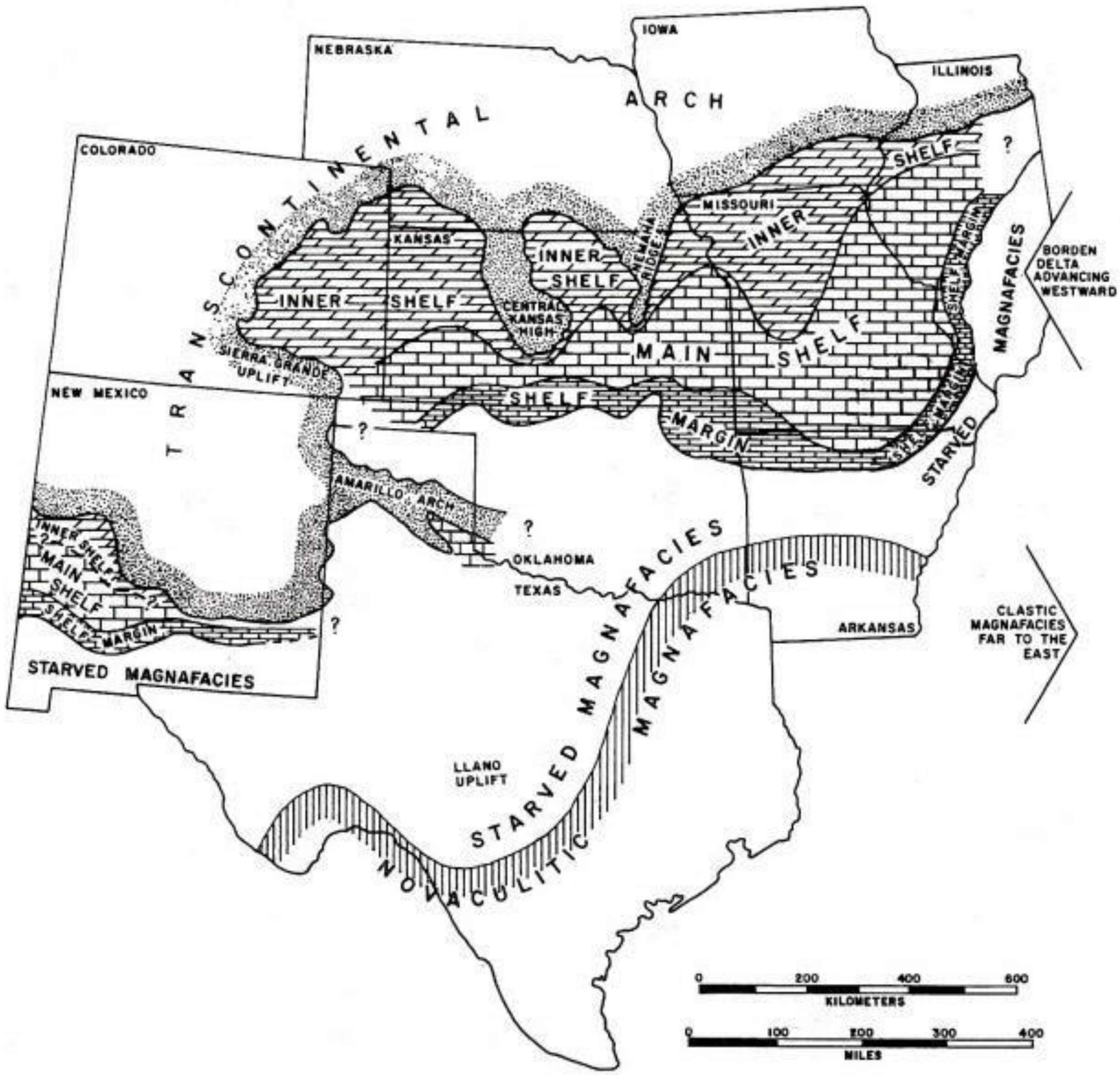

Figure 3. Paleogeogrphic of Arkansas in the Mississippian
Modified paleogeographic map by Manger from Lane and DeKeyser (1980). Generally the Boone Formation is deposited on a shelf margin or ramp. Gutschick and Sandburg (1983) paleogeographic map place Arkansas is approximately 20-30 degrees south from the equator.

limestones during the Carboniferous in ramp setting that illustrate carbonate transport, have been documented in numerous studies (Bachtel and Dorobeck, 1998; Davies, 1977; Lasemi et al, 1998).

The geologic features from studies provide helpful analogues to explain sedimentary structures within the Boone Formation. Carbonate sediment originate from depositional environments that are warm, generally shallow, and clean waters that can be largely effected by: latitude, temperature, salinity, water depth, sunlight intensity, turbidity, water circulation, and nutrient supply (Wilson, 1975; Hansford and Loucks, 1993). General sequence stratigraphic models explain carbonate depositional patterns and geometries are hindered because of its operational principles. The assumption of the sediment being derived from outside of the basin through fluvial or deltaic methods is not fully applicable to carbonates, because carbonate sediments are produced in the marine basin by inorganic or organic processes (Hansford and Loucks, 1993). In addition, when interpreting carbonates the topography of the underlying unit plays a major role in determining geometry, internal structures, composition, and texture of sand bodies (Ball, 1967).

Previous investigation of the Boone Formation include: Davis (2007), Shelby (1986), and Linear (1980). The characterization of the Boone Formation as an aquifer is described in Stanton (1993).

Location and Site Description

The Beaver Lake Quarry and Hindsville Quarry are in the physiographic region of Arkansas known as the Springfield Plateau (Hudson, 2001). The Beaver Lake quarry is west of Eureka Springs, Arkansas and is operated by the Arkansas Corps of Engineers (figure 4). The top of the St. Joe Formation crops out in a small portion of the quarry. The Hindsville quarry is operated by APAC Arkansas McClinton Anchor and located in the northeastern portion of Washington County (figure 5). Permission is needed to access the Hindsville Quarry and an assistant is needed while doing fieldwork.

Terrestrial LiDAR

The Center for Advanced Spatial Technology (CAST) at the University of Arkansas, Fayetteville provided the equipment and advisefor the Terrestrial LiDAR scan. All terrestrial laser scanning (TLS) works in a similar manner, "a laser pulse leaves the instrument in a known direction, travels to a remote target, bounces off the target, and returns to the instrument" (Bellian, et al, 2005). The return time of the reflection of the laser pulse allows the calculation of the distance. These distances are then converted from a spherical to a Cartesian coordinate system as a point in space that lies on the scanned surface. The collection of range measurements and the orientation are in a data set called a point cloud. A mesh formed from the aligned points serves as a basis for the digital outcrop model (DOM). Terrestrial LiDAR is a remote sensing tool that creates a dense point cloud of a surveyed object.

Terrestrial laser scanning allows quantitative and qualitative methods of investigation. LiDAR allows the improvement of current field methods by quantifying observations and visually capturing information visible and invisible to the human eye (Bellian, et al, 2005). Algorithms can be applied to high resolution terrestrial LiDAR scan to extract fracture orientation and assist in the identification of the outcrop fracture pattern (Olariu et al, 2008; Wilson et al, 2011). The architectural style and relationship between facies can be further understood with the investigation of terrestrial LiDAR (Perez et al, 2010). The spectral capabilities of LiDAR allow the discrimination between certain lithologies and quantify stratigraphy through normalized intensity returns (Burton et al, 2011; Franceschi et al, 2009).

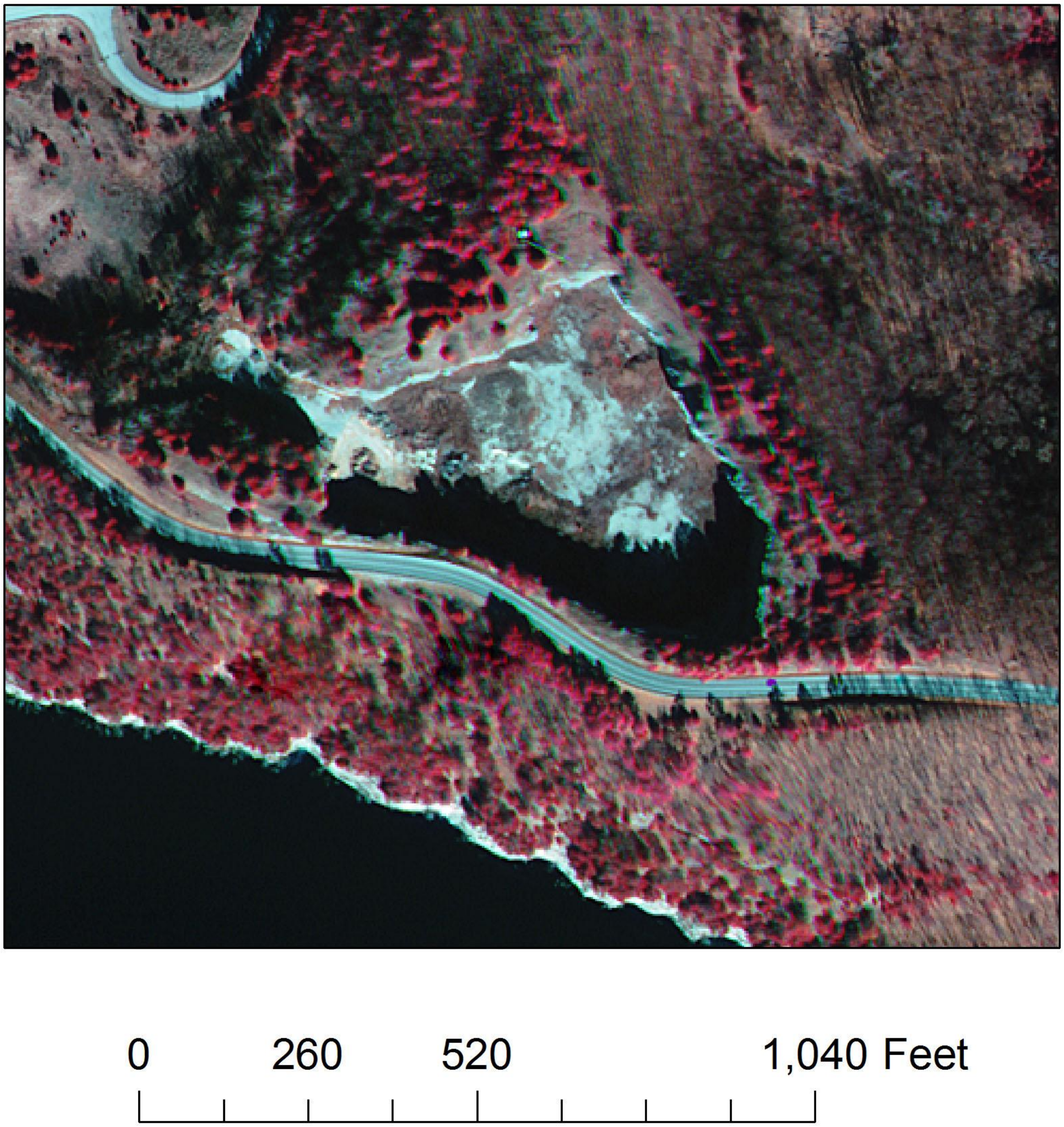

Figure 4. Beaver lake Quarry
The Beaver Lake quarry is located in the southeast corner of Beaver quadrangle. The above is a subset of the southeastern Beaver Digitial Orthophoto Quarter Quad (DOQQ) of the Beaver Lake Quarry. The quarry is operated by Arkansas Corps of Engineers and quarry is approximately 75-80 feet high.

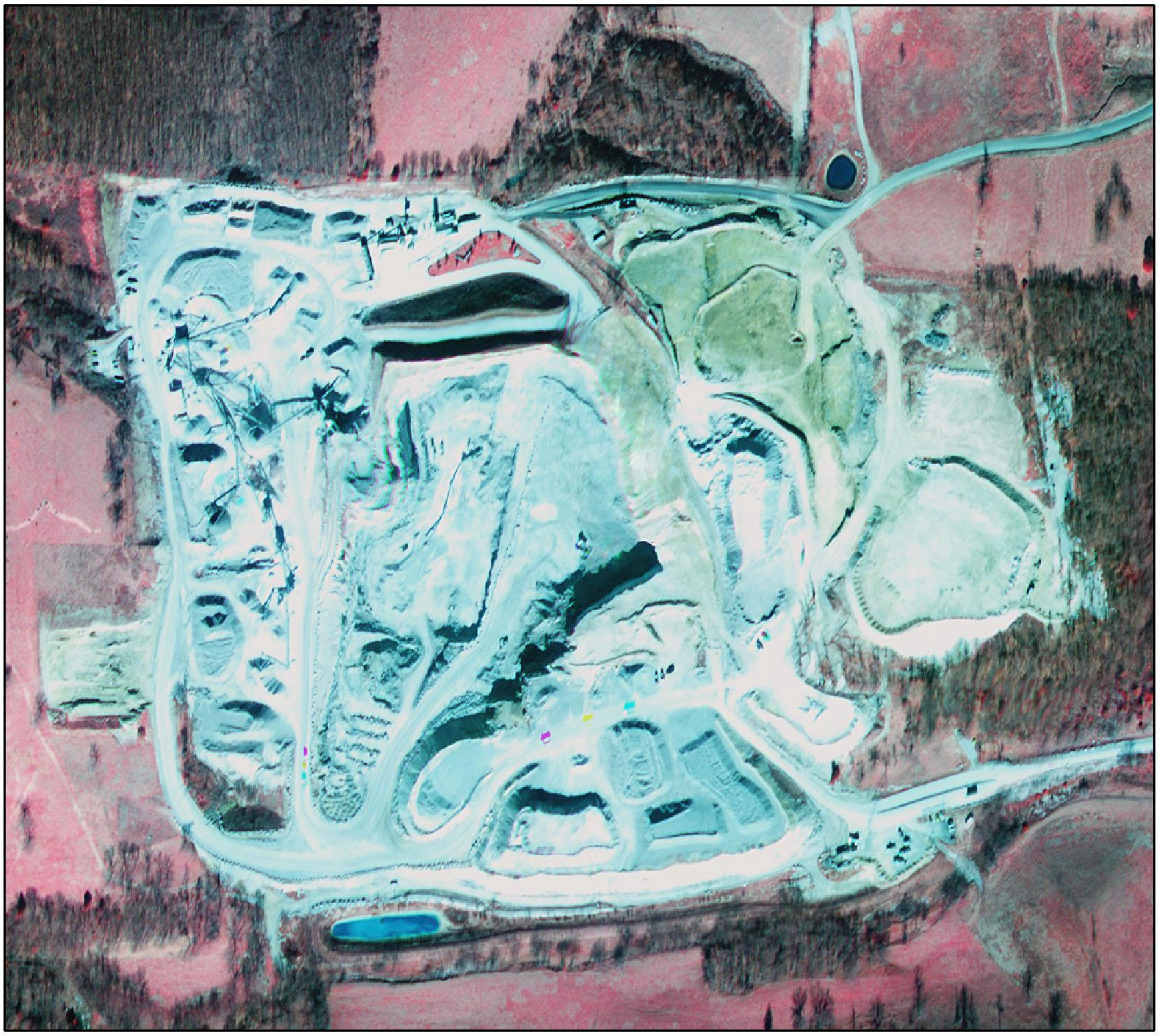

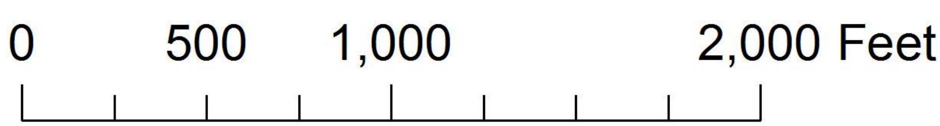

Figure 5. Hindsville Quarry
The Hindsville Quarry is located in the southwest parcel of the Spring Valley quadrangle. The above is a subset of the southwestern Spring Valley DOQQ of the Hindsville Quarry. The quarry is operated by APAC and quarry walls can be as high as 114 feet.

Terrestrial laser scanning is used in numerous applications to document and extract range measurement in a multitude of settings. The power of the backscatter of the laser is recorded into a value referred to as the intensity. Distance and incidence angles are the largest effect of intensity values and the correction of the effects are possible (Kaasalainen et al, 2011; Pfeifer et al, 2007). An empirically derived equation that arbitrary normalizes intensity data will provide a higher quality data set.

Purpose and Scope

The recent interest in Mississippian strata as potential reservoirs southern Kansas and northern Oklahoma illustrates the need for more research into the geology of the Boone Formation. The recognition and understanding of the Reeds Spring facies in the subsurface is relatively poor and few studies have been published on the formation. Information expanding on reservoir characterization would be beneficial in trying to understand the complexities of the formation.

The objective of this study is to characterize the Reeds Spring facies at the Hindsville Quarry. This investigation will contribute information in the assessment of Terrestrial LiDAR in geologic outcrops, and a stratigraphic framework of the Reeds Spring at the investigated outcrops. The creation of a digital outcrop model allows an easily accessible dataset that can build interest and comprehension of the formation. Outcrop studies can serve as an analogue to the subsurface and further the understanding of the Reeds Spring Formation as a hydrocarbon reservoir. In addition, the information pertaining to fracture patterns is economically beneficial to the geologist working the interval.

Methods

Traditional fieldwork, data acquisition, and data processing are the major components of this project's methodology. Traditional fieldwork in conjunction with photography of the research site, construction and description of stratigraphic columns, facies descriptions, and measurements of the orientation of quarry walls are all utilized. These descriptions will be compared to existing literature and expounded upon.

Sample Collection

Two samples at the Hindsville quarry were collected for three thin section analysis. The samples were collected from two different stratigraphic zones (figure 6). The samples were labeled THQA and THQB where B is stratigraphically older than A. Rock samples were then cut at the University of Arkansas and sent to the National Petrographic Service in Houston, Texas. The thin sections have been impregnated with a clear epoxy to prevent the sample from fracturing. The thin sections are covered in clear nail polish to act as a temporary cover slip.

Photography

Canon EOS 5D and Nikon D60 cameras were used at each site to capture raw format images in high resolution. The majority of photos were taken around 35mm to avoid distortion and compression. The photos are used to create photo mosaics to highlight geologic features within the Hindsville Quarry.

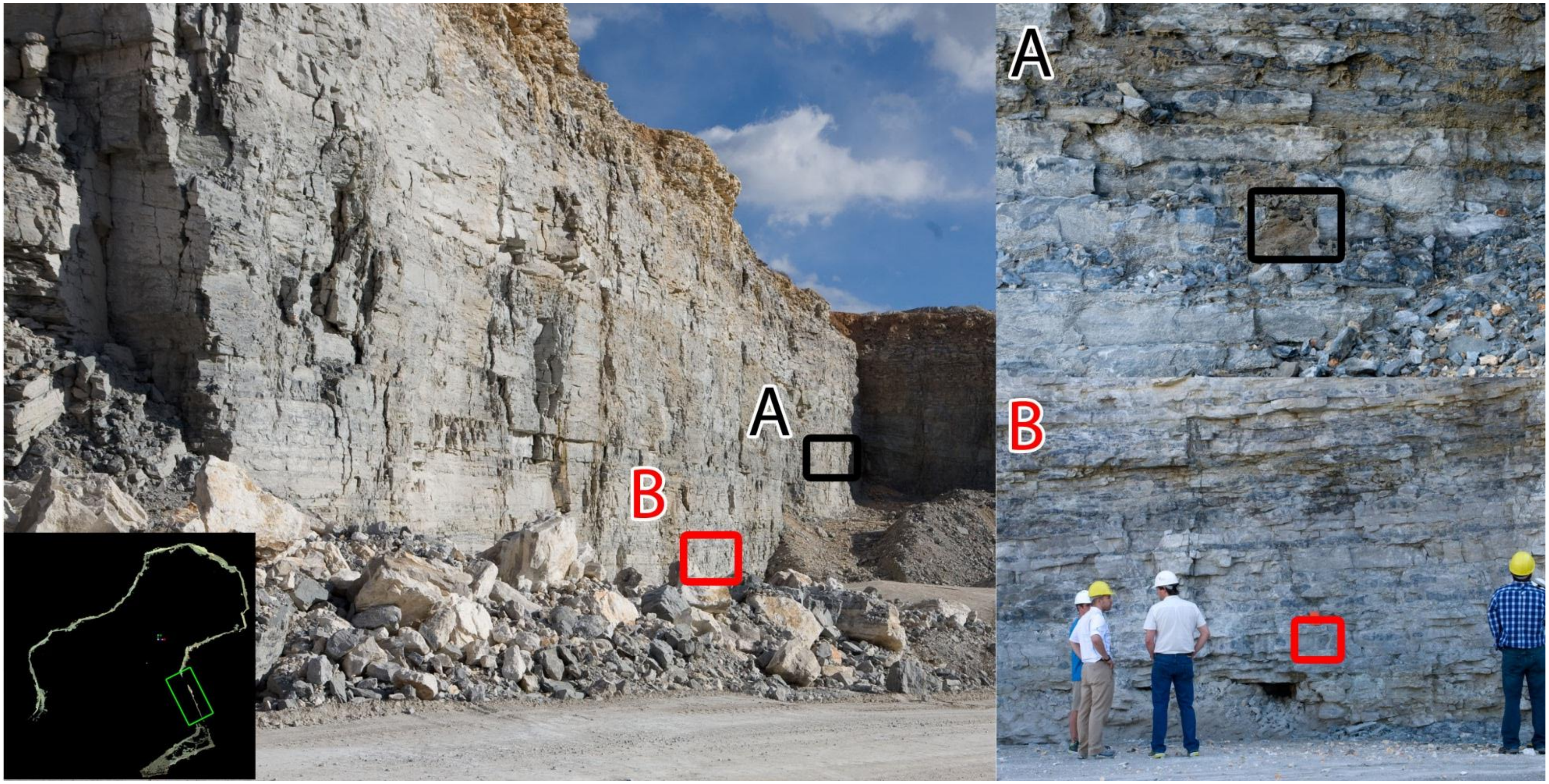

Figure 6. Sample Collection Location
The collection of two rock samples are collected at two different localities to assist in geologic understanding of the outcrop. Sample THQB (B) is stratigraphically younger then sample THQA (A).

Terrestrial LiDAR

Data acquisition involves the use of Terrestrial LiDAR scans, particularly time-of-flight (TOF) scanners and phase-based scanners. TOF scanners are mostly based on LiDAR principals while phase-based scanners operate similarly to total stations. In general, TOF scanners operate at longer ranges but slower rates compared to phase-based scanners. The LiDAR scan will be conducted by CAST, led by Dr. Jack Cothren and Malcolm Williamson. The outcrop scans were accomplished with the Lecia C10 (1), Optech ILRIS 3-D (2), and Z+F 5006i (3) (figure 7).

Terrestrial LiDAR Equipment

1. The Leica C10 Scan Station scanner is a time-of-flight scanner with an effective operating range of 1-200 m (up to 300 m with 90% reflectivity in the 530nm wavelength of its laser). Its motorized head allows scanning of a complete 360 degree by 270 degree area. Data is acquired at a rate of 50,000 points/second and can be stored on-board or on a wireless or wired laptop. The C10 has a number of features that make it particularly effective. For example it has automatic target acquisition capabilities that quickly allow survey control points to be integrated to the scan data. CAST has a number of targets for this purpose. The C10 has an on-board digital camera that can be used for scan management/planning and is automatically aligned with the scans to texture the point clouds. Published specifications indicate that the accuracy of a single measurement is 6 mm in position and 4 mm in depth (at ranges up to 50 m). The system supports traverse and resection capabilities and can be integrated with a companion Leica GS15 GPS receiver.

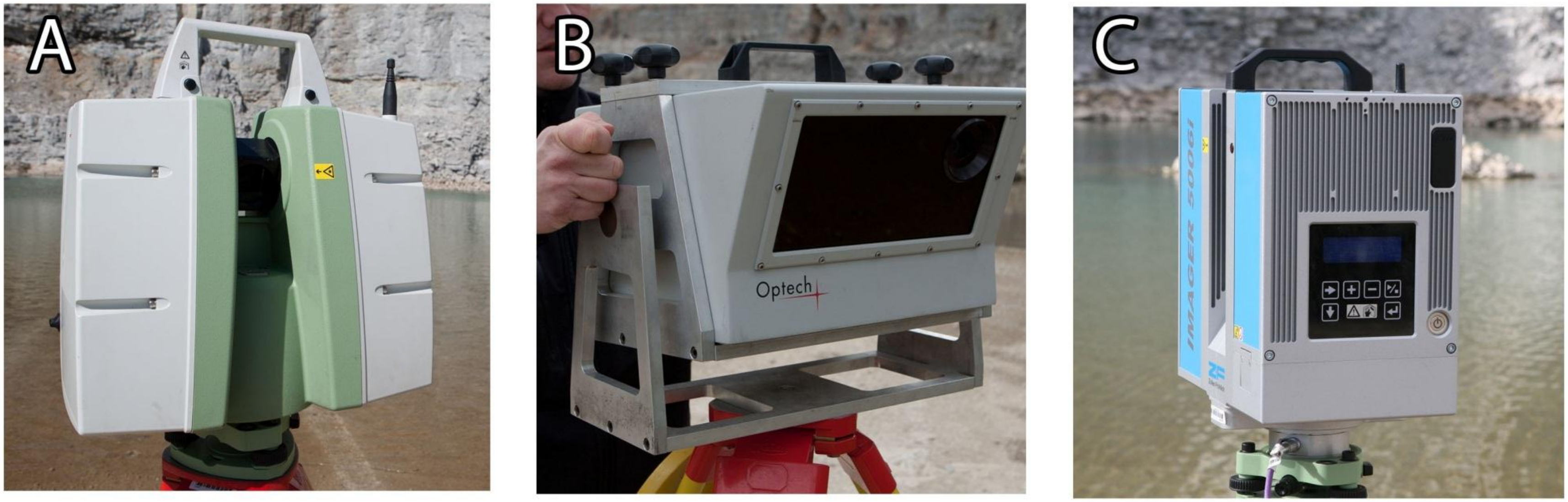

Figure 7. Terrestrial Laser Scanning Equipment
A) The Leica C10 Scan Station Scanner is the main scanner used at the Hindsville quarry scan. The C10 is a time of flight scanner, with a 530nm wavelength, and able to acquire points at a rate of 50,000 points per second. B) The Intelligent Laser Ranging Imaging System (ILRIS-3D) was used at the Hindsville Quarry for latter comparative uses. C) Z+F scanner is the main scanner used at the Beaver Laker preliminary study. The scanner is an inferred phase base system, has an infrered wavelength at 1500nm, and can acquire data at a rate up to 500,000 points per second.

2. The Intelligent Laser Ranging Imaging System (ILRIS-3D), manufactured by Optech, Inc., is an imaging system that offers direct-to-digital 3D models of any scene. The scanner is about the size of a motorized total station, with on-board digital camera and large-format LCD viewfinder. The ILRIS-3D has a visual interface similar to that of a digital camera. The unit is portable, weighing 12 kg and can easily be used in the field by a single person. As the laser is Type 1, it can be safely used in all settings. With a 20% reflectance surface (near the 1500nm wavelength of its laser) it has a range of 3m – 1 km. Accuracy in the x, y and z dimensions is +\- 10 mm at 100 m. Point cloud data are captured at 2000 points/second. A typical scene with adjacent point spacing can be fully scanned in 10-15 minutes, capturing 1.2 to 1.8 million points.
3. The Z+F 5006i scanner is an inferred phase based system, thus allowing very rapid data acquisition at up to some 500,000 points/second. The Z+F effective working range is 1 meter to 50 meters – though longer distances are possible out to its design limit of 79 meters. The motorized head permits data to be acquired in a 360 degree by 310 degree coverage. The Z+F can be used in stand-alone mode or with wireless or wired connection to a laptop.

<u>Beaver Lake Quarry Scanning Procedure</u>

The Beaver Lake Quarry scan occurred on October 29, 2011 using the Z+F 5006i scanner. Scanning initially focused on the southern face of the quarry wall, and subsequent scans are from three different perspectives, approximately 18 meters from the wall face. The two ground scans and one scan from the boom were set up to take 360-degree view scans of the quarry.

The purpose of the Beaver Laker Quarry scan was to gain perspective on future scans and the abilities of the scanner on a geologic outcrop. The scan was done in low resolution; angle and distance played a large role in the quality and intensity returns of the data. Although the resolution is of low quality overall the wall in front of the scanner produces an image where bedding and stratigraphic pattern can be interpreted. Generally, limestone and chert can be visually distinguished in the hue intensity data (Figure 9). Cyclone transforms the Intensity data to an interval from 0 to 1 based on maximum and minimum values of the imported data set. These maximum and minimum values correspond to the max and min of the color map applied, thus trying to aid the user in visualization. A numerical range of values has not been established to make this evaluation in the raw data. In addition to the scan, numerous photos were taken to document the quarry.

Hindsville Quarry Scanning Procedure

Hindsville Quarry scan occurred on February 24, 2012 with ILRIS-3D, Z+F 5006i, and Leica C10. The northwestern face with intricate stratigraphic pattern is the focus of multiple scans within Hindsville quarry (Figure 10). The Leica C10 is the main scanner in the evaluation and interpretation of the geologic outcrop. Four scans were completed using the Leica C10 and one scan each were made with the ILRIS -3D and Z+F 5006i. Location 2 is the location that all three scanners were set up for comparison purposes.

The Leica C10 scanner collected three scans from three different locations on the northwestern face (figure 11). The scanners at each location were first leveled manually on tri pod and then the C10 internally leveled itself. Location 1 has a scan resolution of 1 cm at 108 meter, the upper left corner and lower right corner of the scan were picked manually on the C10

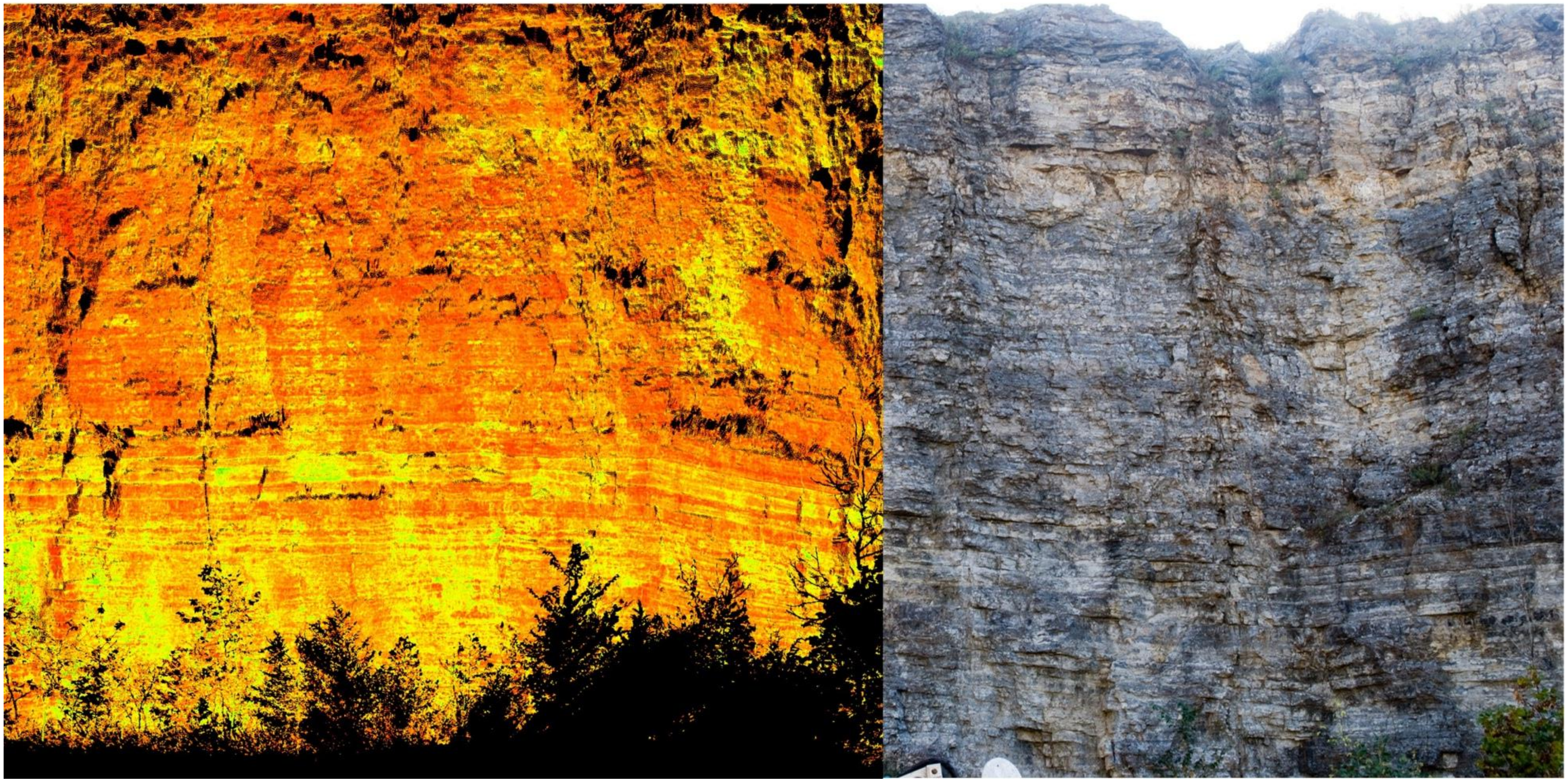

Figure 9. Terrestrial LiDAR and Photo Comparison at Beaver Lake
The Photo and the Terrestrial LiDAR scan depicts the east most portion of the southern wall of the Hindsville quarry. Within the image the bedding plates, stragraphic pattern, and different lithologies (chert and limestone) can be distinguished. The different colors correspond to variety intensity returns.

Figure 10. Northwestern wall located at the Hindsville Quarry
The study will focus the assessment of Terrestrial LiDAR on the northwestern wall of the Hindsville Quarry. The wall is the location of the most intricate stratigraphic pattern seen in the Boone Formation.

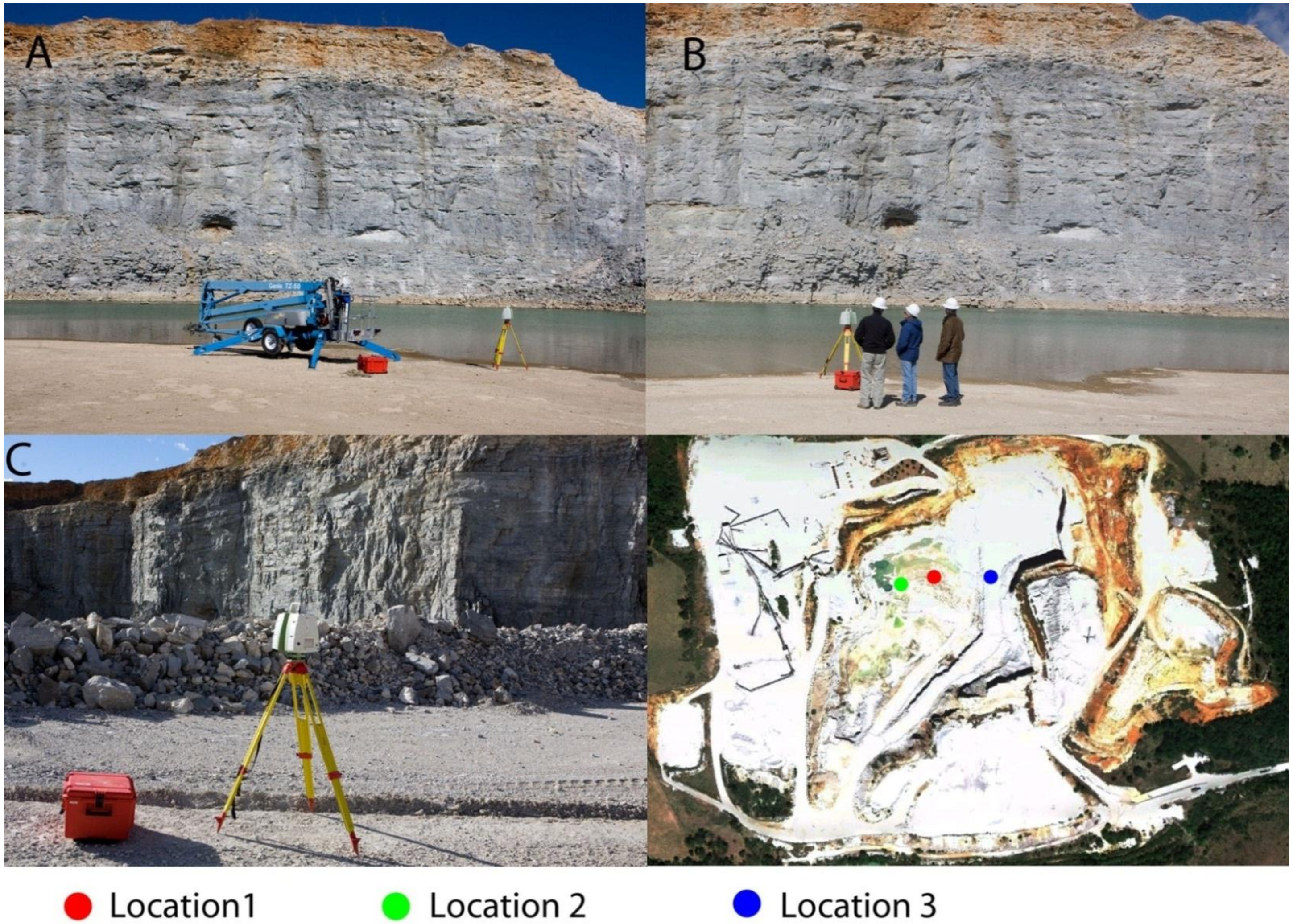

Figure 11. Location of Scan Position in the Hindsville Quarry
The Terrestrial LiDAR scanning scanned the northwest quarry wall from three different localities. A) Location 1 B) Location 2 C) Location 3. Each scan is set to take a resolution of 1 cm between each point and took approximately 70 minutes per scan location.

scanners LCD screen.   Photo resolutions of 1920x1920 were chosen for scans for location 1 and 2. Location 4 is the location of the 360-degree scan completed with medium resolution.

The orientation of different wall faces was done with a Burton compass, Google Earth, and Scan 4 of the terrestrial LiDAR scans. A number of faces in the quarry are inaccessible, therefore the alternative methods of Google Earth and terrestrial LiDAR were used to determinethe orientation of inaccessible wall faces. The ruler tool in Google Earth allows the measurement of orientation, and these values were compared to field measurements of accessible walls in the Hindsville quarry. The top view of scan 4 was exported as an orthophoto and walls were compared for similar orientation. Thus the orientation of inaccessible wall faces was generally established through an indirect comparative method.

Data Processing

The processing of the scan was accomplished using Leica Geosystems' Cyclone 7.3 software workflows of the following process and it can be found at http://gmv.cast.uark.edu/category/Cyclone-workflows/. Cyclone is software package in which data can be visualized, navigated, measured and modeled. Data imported into Cyclone removes vegetation and other infringing objects. The different scans are tied together by linking two scans together at a time by matching 3 constraining points, this process is known as registration (figure 12). The Error Vector/RMS error from the constraint optimization should be around .01 meters, and a tied together scan will then be matched to another scan until all quarry scans are aligned. The aligned scans are then meshed using techniques that can be as simple as Delaunay triangulation or as complex as surface using radial basis functions taking into account the uncertainty of the individual points in the cloud.

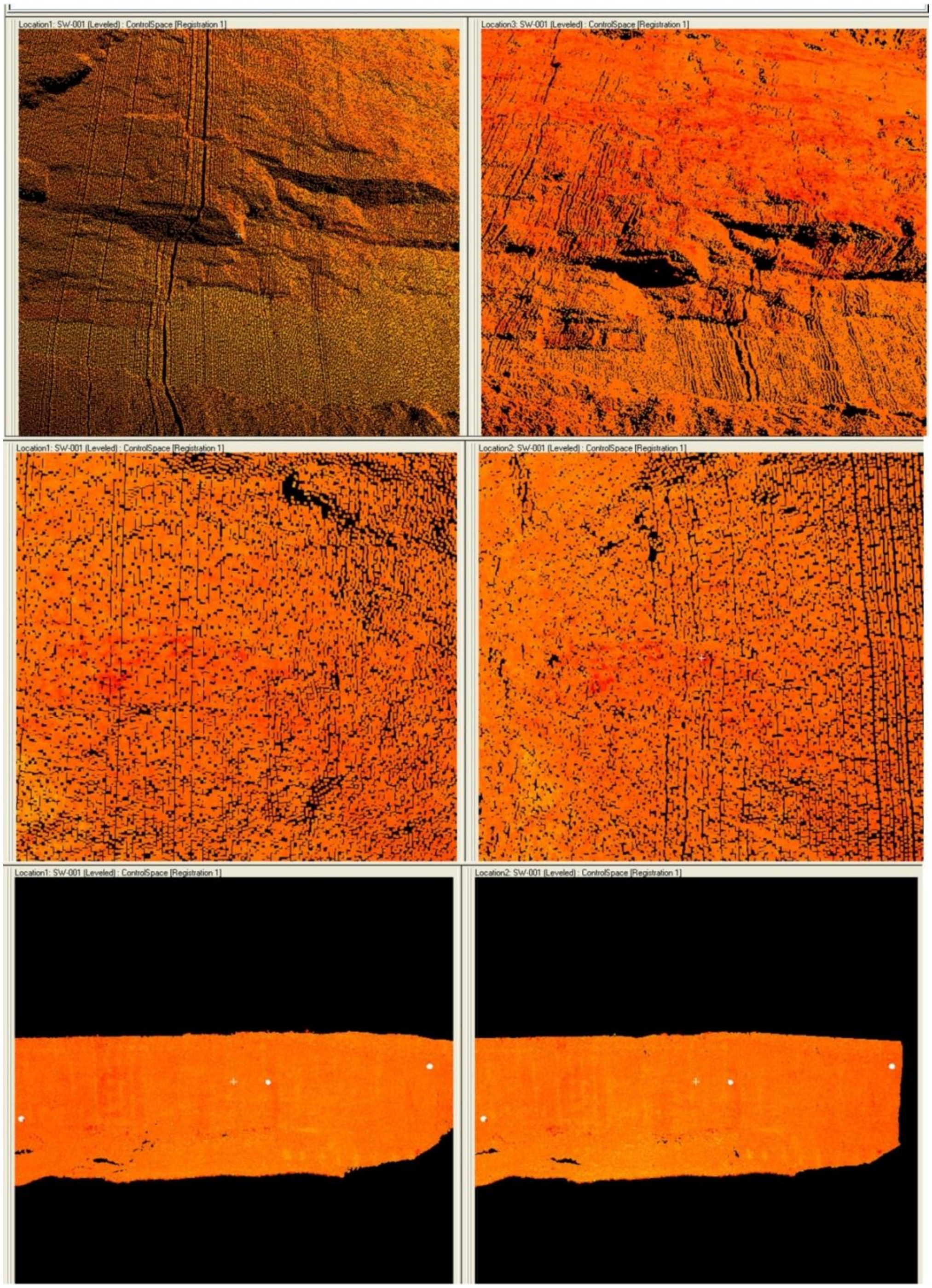

Figure 12. Registration Process

The registration is the process of tying two scans together at a time by finding similar features in each scan. The color intensity map is the most useful when registering scan, intensity values help outline geologic features within the scan.

Beaver Lake Quarry

All three scan have been processed and only two of the scans could be registered. The third scan from the boom presented too much variability because of wind moving the scanner during scanning.

Hindsville Quarry

The Leica C10 scans were imported, cleaned up, and registered using Cyclone 7.3. All scans have been registered together and each scan averaged an RMS error of .01 meters. The Registrations of multiple scan allows the reduction of data shadow (blank spots in the data, because of angle of the laser scanner), thus allowing a better interpretation of stratigraphic patterns and bedding planes. The fourth scan was cleaned up and assisted with orientation of different quarry walls that could not be measured with a compass.

The cleaned LiDAR scans were used to create stratigraphic columns and interpret the stratigraphic architecture. LiDAR scans allow accurate measurements since each point recorded can allow measurement from the scanner and between individual points. Orthophotos were exported with measurements on them to help facilitate measurement in a different program.

The orthophoto photo was open in Adobe Photoshop to outline stratigraphic patterns, bedding planes, and surface boundaries. The interpretation of beds and stratigraphic zones were a combination of the LiDAR image in Cyclone and photographs taken in the field.

Matlab (R2012a) is a program for algorithm development, data analysis, visualization, and numerical computation. Simple algorithms to normalize, plot, and cluster exported sections of the LiDAR data (appendix 1). Cyclone data is exported as a pts file where x, y, z, coordinates, intensity values, and RGB values from the camera are a part of the file. The coordinates system "correspond to the center of the vertex or sphere," thus corresponding to the scanner. A general statistical assessment of the data set was accomplished using different algorithms in Matlab.

The data showed an inversely proportional relationship with intensities and distance (figure 13). Data was normalized arbitrary by maximum and minimum values of the Intensities (figure 14; Appendix A). A function operations polyfit and polyeval were used to calculate a second degree polynomial of intensity versus distance using least squares. The residuals of the calculated polynomial and raw data were then calculated. The minimum and the maximum values of the residuals were used in a system of equations to scale the data between 0 and 255. The solved values of slope and intercept were calculated and used to normalize the data with respect to distance.

The incidence angle calculation and correction was done using a script in Matlab (Appendix A). The dataset was subset for every 1000^{th} point for easier process, and an index was created to reference each point in a particular range. For each point, a plane was assessed based on a number of points in a particular radius. The cosine of the incidence angle is calculated by calculating the dot product of the plane normal and the normal of the individual point. The normalization of the incidence angle is calculated by the division of the normalized distance by the cosine of the incidence angle. Terrestrial LiDAR is largely effected by distance, incidence angle, and reflectance of the material being scanned. The normalization of distance and incidence angle eliminates those components and intensity data is then largely based on reflectance of the material

Clustering the data was accomplished by an unsupervised clustering method within Matlab (Appendix B). The unsupervised clustering was done with k-means into a number of classes that optimized visualization of the dataset. K-means is an algorithm that partitions the points in a matrix into a selected number of clusters based on squared Euclidean distance from a centroid of a cluster.

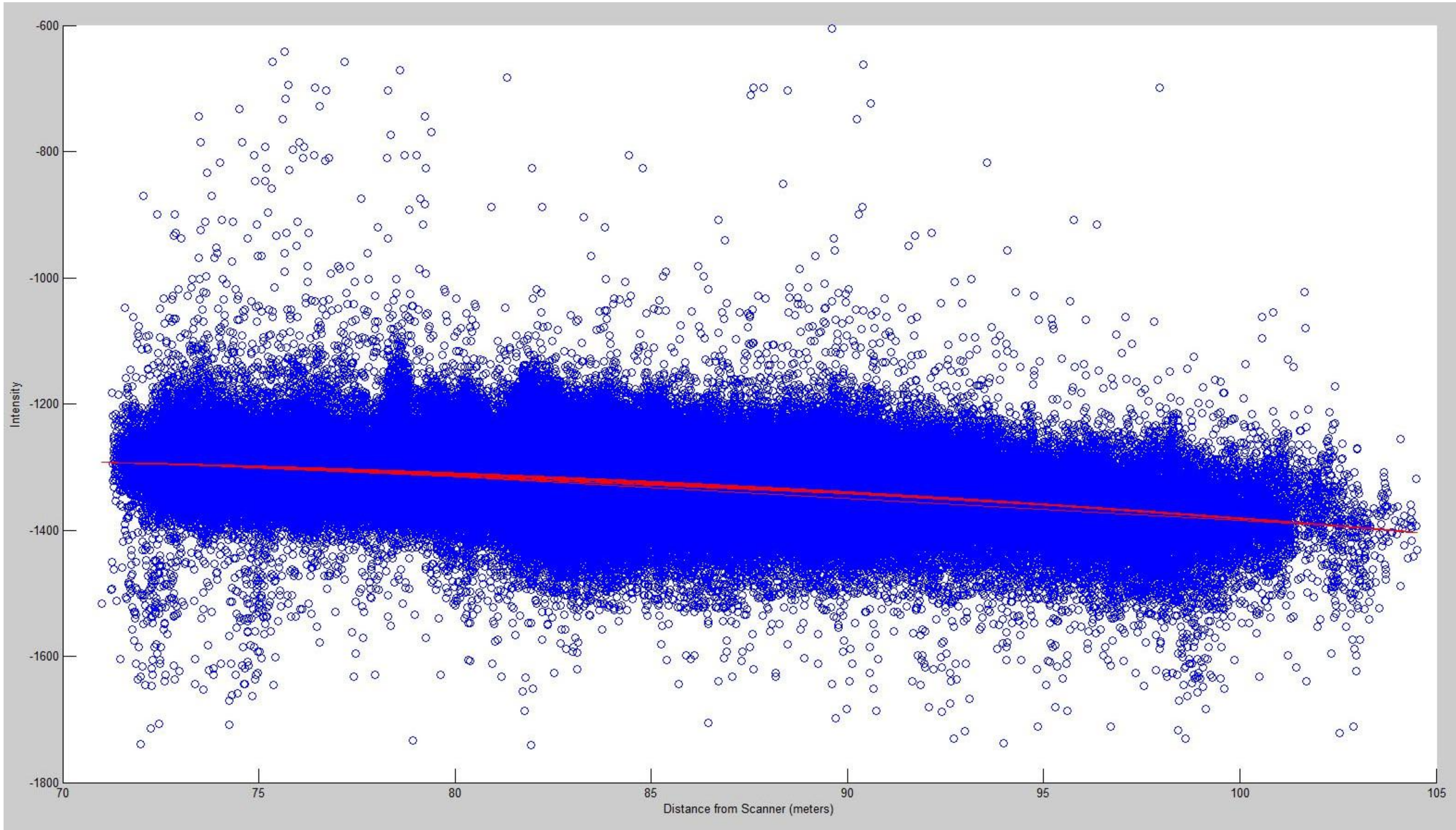

Figure 13. Raw Intensity data relationship with distance from the scanner
The data is a graph of raw intensity returns versus distance from the scanner (meters). The data shows a decrease in intensity returns as an increase in distance. Therefore the data needed to be normalized. The red line depicts the fitting of a second degree polynomial to the data set. The below is the equation of the line fitted to the data.

-0.057 x^2+6.7x-1481

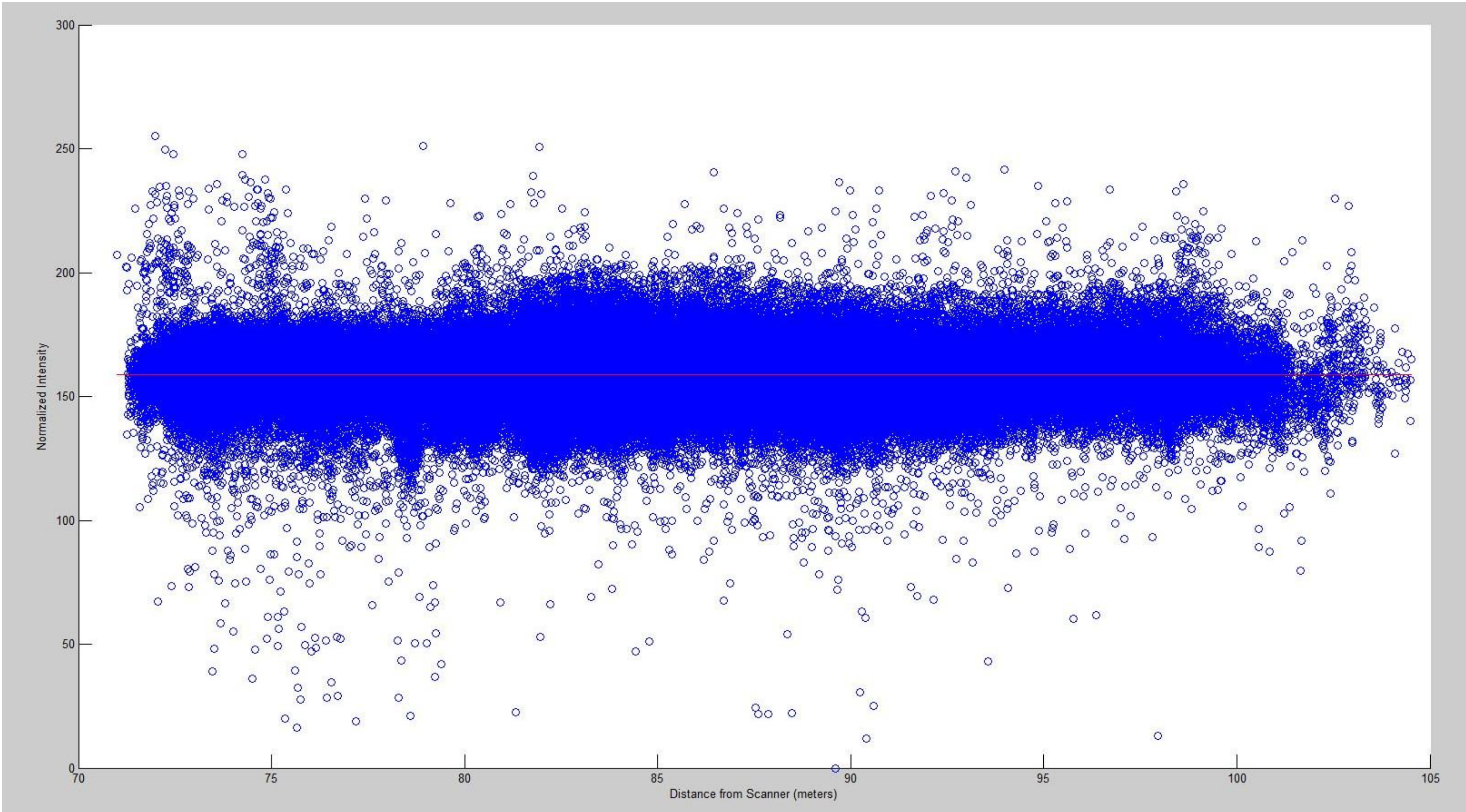

Figure 14. Normalized Intensity Data
The data set is normalized with minimum and maximum values of 0 and 255. A second degree polynomial and raw intensity data was used to calculate the residuals. The residual and max and minimum values were used to create a system of equation. The solved variable of the system of equation was used in an equation to calculate the normalized intensity values.

Results

Lower Boone, Upper Boone, Tripolitic Chert, and regolith are present at the Hindsville Quarry (figure 15). In the quarry there are indications of truncated surfaces and angular relationships between bedding surfaces (figure 16). The stratigraphic patterns and lithology highlighted within this section reflect transported carbonates (transportation could be through traction current, storm wave, tidal waves, turbidity currents or lobate manner). The northwest wall is the focus of the study and the quarry face can be broken up into six different zones. Within the quarry there are three significantly readily identifiable surfaces that can help with stratigraphically orienting oneself, thus allowing a better understanding of stratigraphic architecture (figure 17).

The terrestrial LiDAR scans, photos, and surrounding equivalent sections at the Hindsville quarry were used to establish six different zones on the northwestern wall of the quarry. The zones are classified by stratigraphic pattern, bedding, and lithology. Zone 1 is an even parallel medium bedded limestone. Zone 2 is a wavy nonparallel medium to thinly bedded limestone with anastomosing dark chert interbedded with very thin lamina of discontinuous clay. Zone 3 is a parallel medium to thinly bedded limestone with interbedded discontinuous bedded dark chert. Zone 4 is low angle cross and curved nonparallel medium bedded limestone with interbedded dark chert. Zone 5 is a lightly weathered discontinuous curved nonparallel limestone. Zone 6 is a highly weathered discontinues even parallel cherty limestone composition.

<u>Petrography</u>

THQB-1 is from a light grey limestone from zone 3. The allochemical constituent are dominated by crinozoan and bryozoan detritus and is considered to be grain-supported (figure 18).

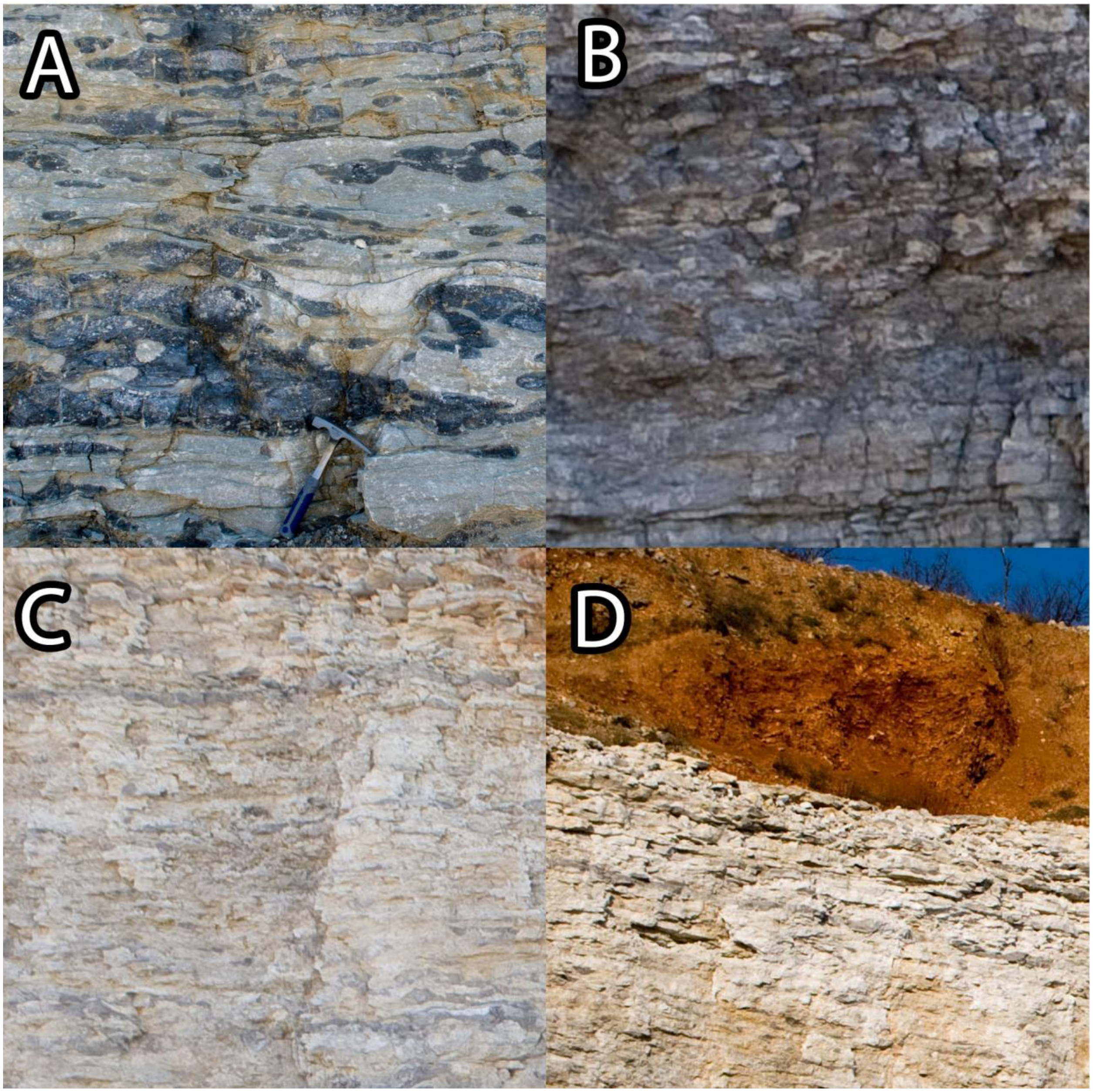

Figure 15. Different Lithologic Units within the Hindsville Quarry
Four pictures showing different lithologies in the area the Hindsville Quarry record the presence of lower Boone, upper Boone, tripolitic chert , and regolith. A) The lower Boone within the study are B) the upper Boone C) tripolitic chert D) regolith

Figure 16. Truncated or Angular Relationships in Hindsville Quarry
The truncated surface and angular relationships are suggestive of transported or carbonate sediments being effected by storm waves.

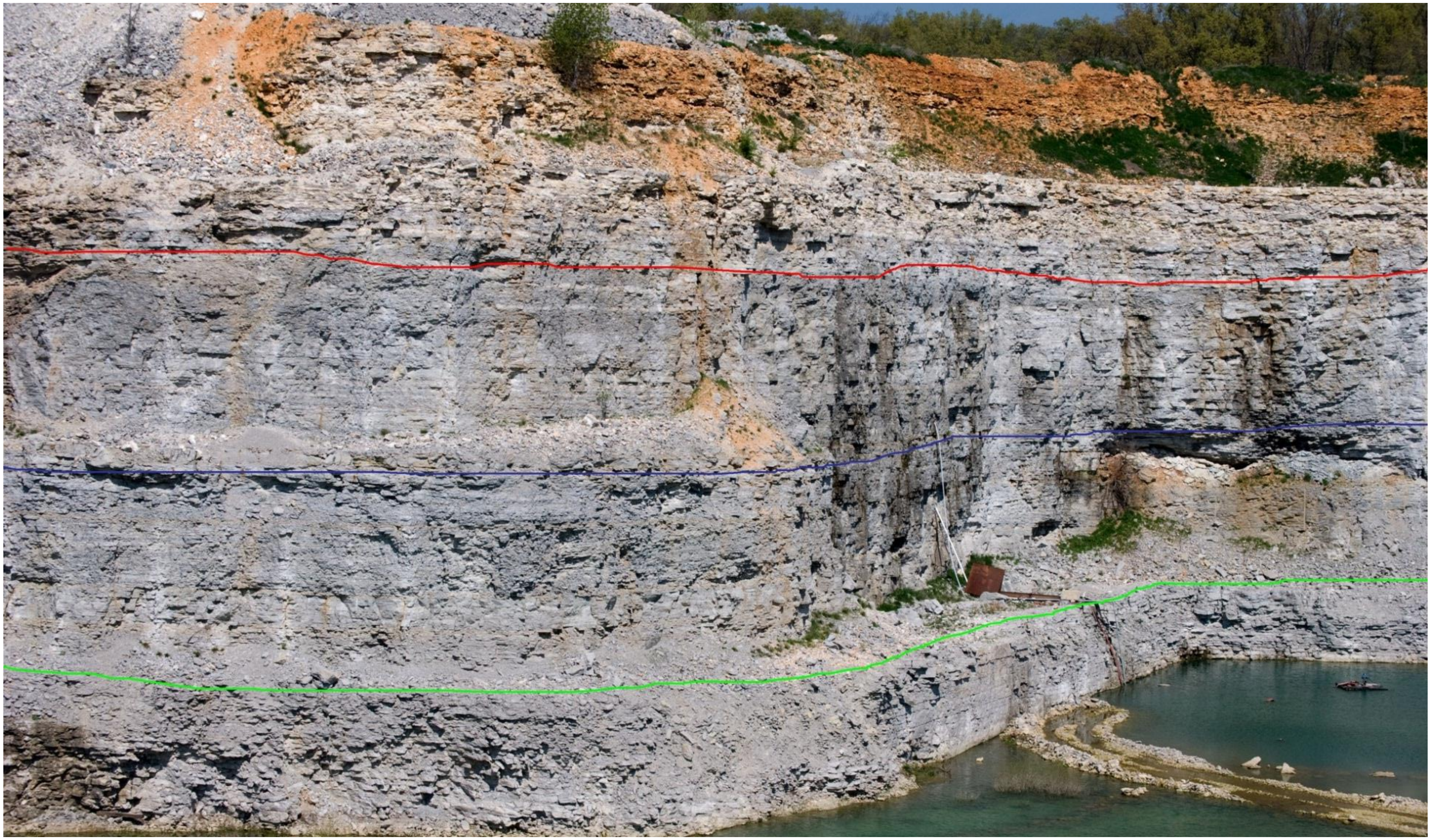

Figure 17. Readily Identifiable Bedding Surfaces
Throughout the Hindsville Quarry there are 3 distinctive bedding surfaces that can be identified.
These surfaces help correlation and understanding of the stratigraphic architecture within the quarry.

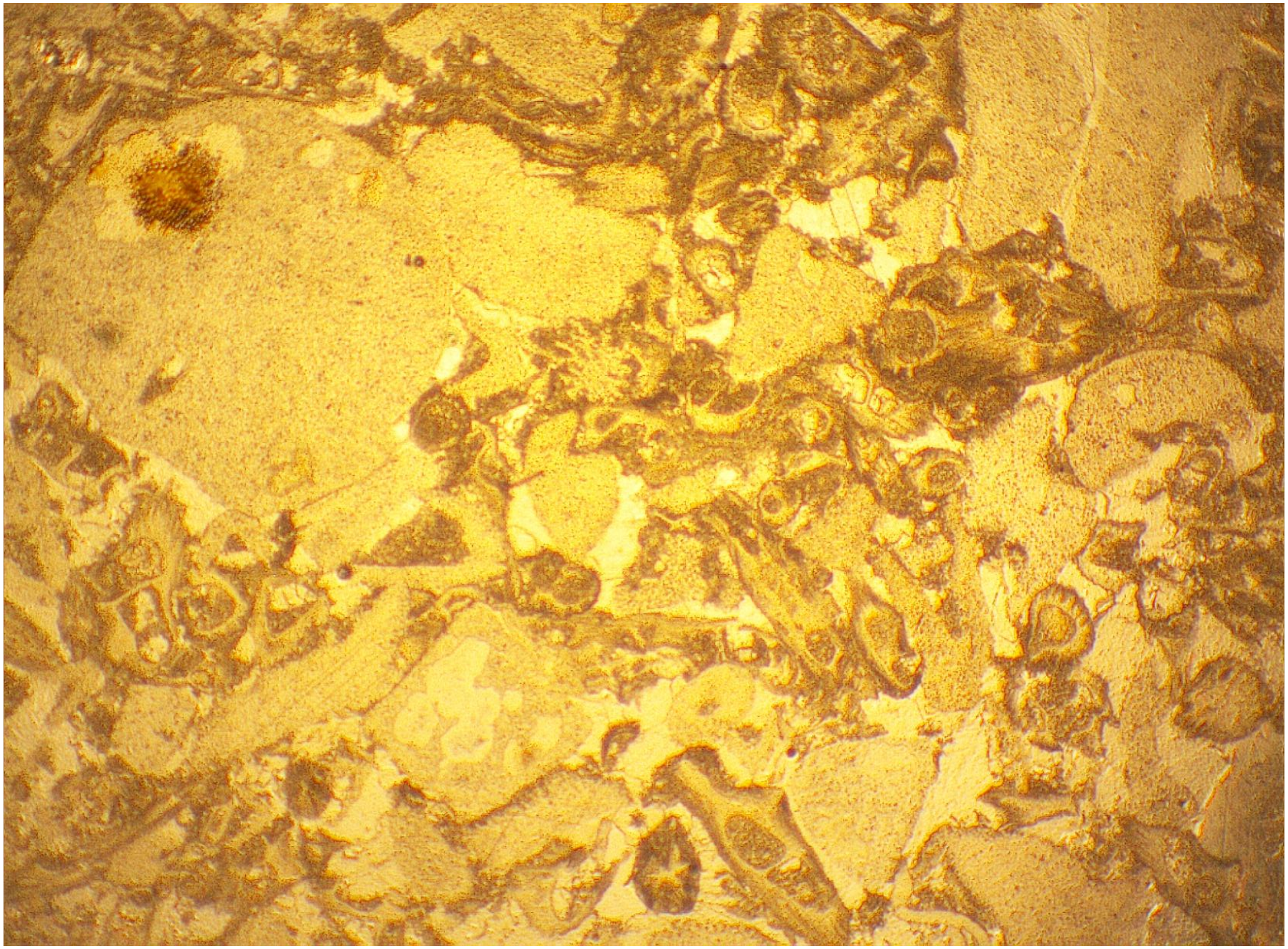

Figure 18. Byrozoan-Crinozoan Lime Packstone
The above image has a length of .025mm across. The sample is grain-supported and dominated by allochemical detritus of Byrozoans and Crinozoans.

This rock fits into Selby's (1986) description of the mixed byryozoan-crinozoan lime packstone subfacies.

Samples THQA-1 and THQA-2 are from one sample from zone 4 separated by a very thin lamination of silt. The sample shows very small fractures and a grading upwards of grains (figure 19). The stratigraphically lower thin section THQA-2 is mud-supported, and allochemical constituents include sponge spicule and crinozoan detritus (figure 20). This thin section fit into the fossil lime wackstone facies description of Shelby (1986). THQA-1 is a grain-supported with the presence of bryozoan and crinozoan detritus (figure 21). The thin section fits into the fossil Lime grainstone faceis described by Selby (1986).

Terrestrial LiDAR

The four Terrestrial LiDAR scans helped identify and analyze the geologic features found in Hindsville Quarry (figure 22). Location 1, location 2, and location 4 provide textural photographic overlay and Intensity returns. Location 3 only has the Intensity return used for visualization because of user error. Figure 23 shows the outputs of the survey of the northwest wall in Hindsville Quarry and the different visualization capabilities within Cyclone. Location 4 is a 360 degree view of the quarry and can be used to measure different orientations of the wall face, thus allowing correlation of stratigraphic features (figure 24). These datasets show recognizable features and patterns using color from an onboard camera, hue intensity map, or grayscale intensity map. The registration of multiple scans was able to reduce data shadows and improve visualization and interpretation (figure 25).

The exportation of multiple orthophotos allowed the interpretation of stratigraphic patterns and stratigraphic columns. The stratigraphic interpretations are created with the facilitation of the navigational tools in Cyclone and photographs taken at different angles in the

Figure 19. THQA
The above photo is of rock sample THQA after being cut with a rock saw. The sample shows an increase in gradation and fracturing. The sample was split into two thin sections, the bottom is labeled THQA-2 and the top is THQA-1.

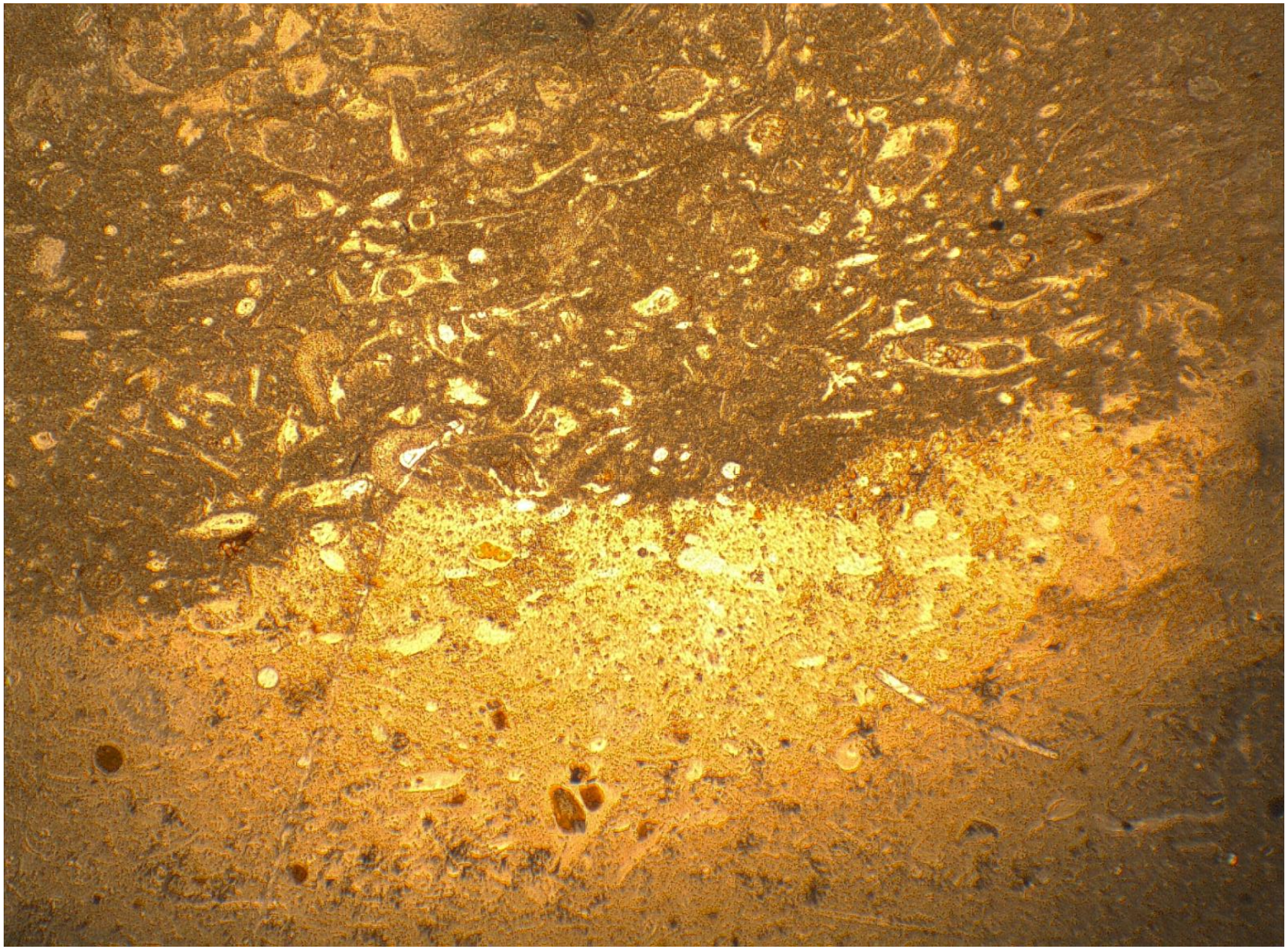

Figure 20. THQA-2: Fossil Lime Wackstone
The sample major allochemical consituents include sponge spicule and crinozoan detritus. The sample also shows a transition of lime into the chert.

Figure 21. THQA-1: Fossil Lime Grainstone
THQA-1 is a grain-supported with the presence of bryozoan and crinozoan detritus. The thin section fits into the fossil Lime grainstone faceis described by Selby (1986).

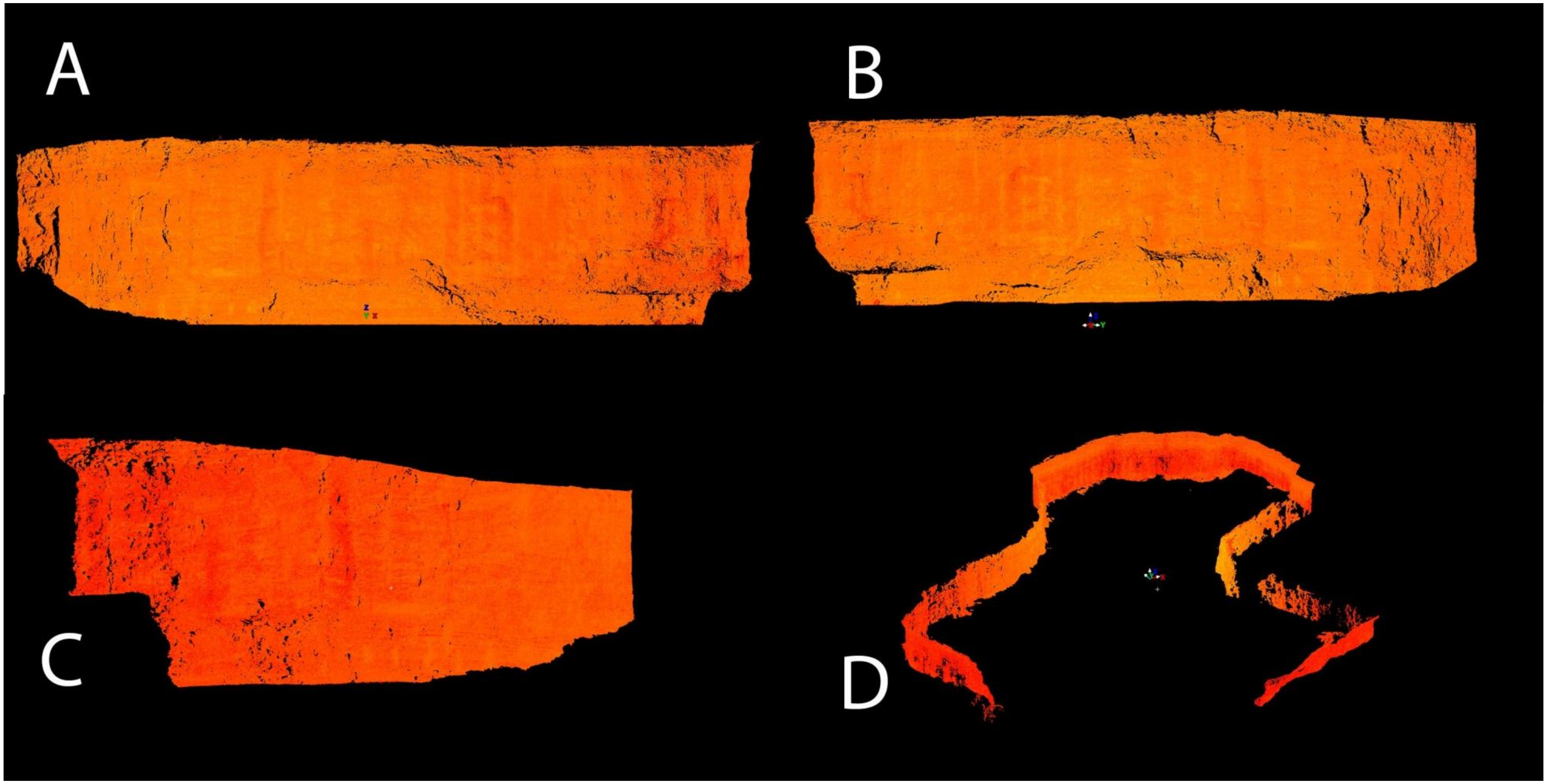

Figure 22. Lecia C10 Scan at the Hindsville Quarry
The four different scan produced large point clouds with all data set. The smallest point cloud (location 4) has 4,577,149 point and the largest (location 2) has 51, 175, 310 points.

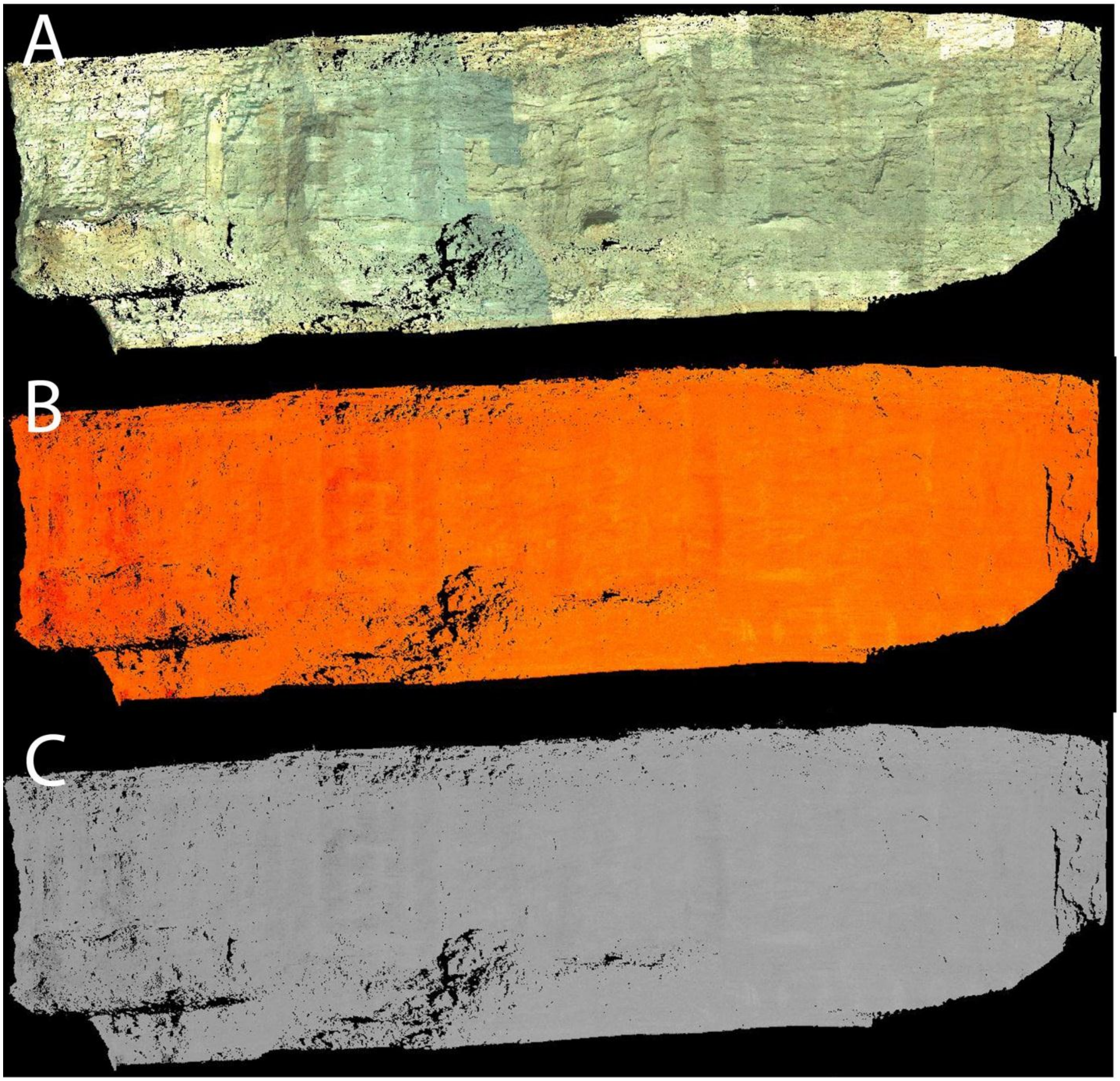

Figure 23. Cyclone Visualization of Scanner data
The spectral capabilities of Terrestrial LiDAR are a major reason of using this remote sensing to asses a geologic outcrop. The C10 allows A) photo texture overlay with intern camera B) Intensity Map in Color C) Intensity Map in Grayscale

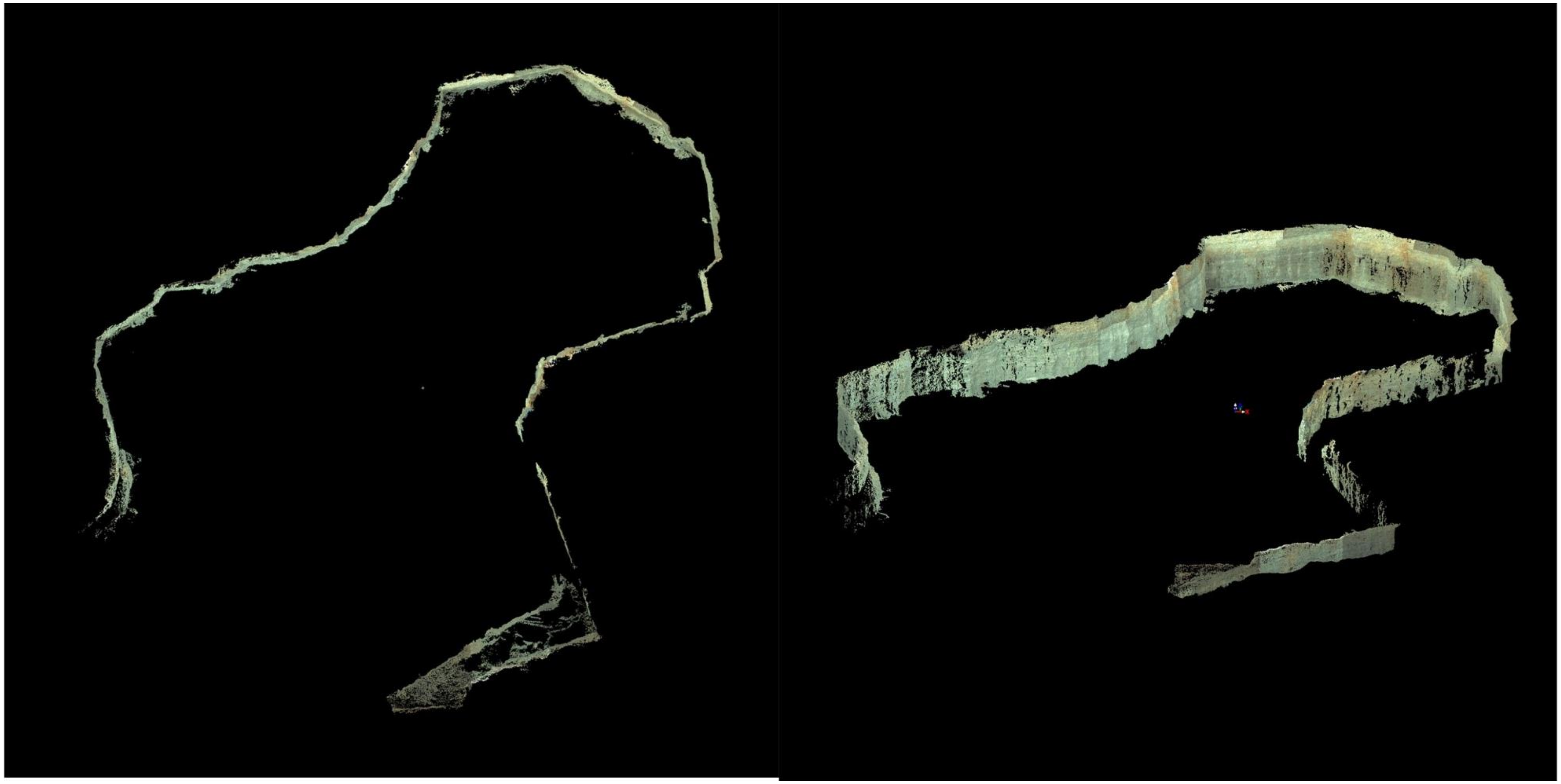

Figure 24.A 360 degree scan of Hindsville Quarry
Scan 4 is the location of the 360 degree scan done in medium resolution. The scan main use is to help correlate the orientations of opposing walls.

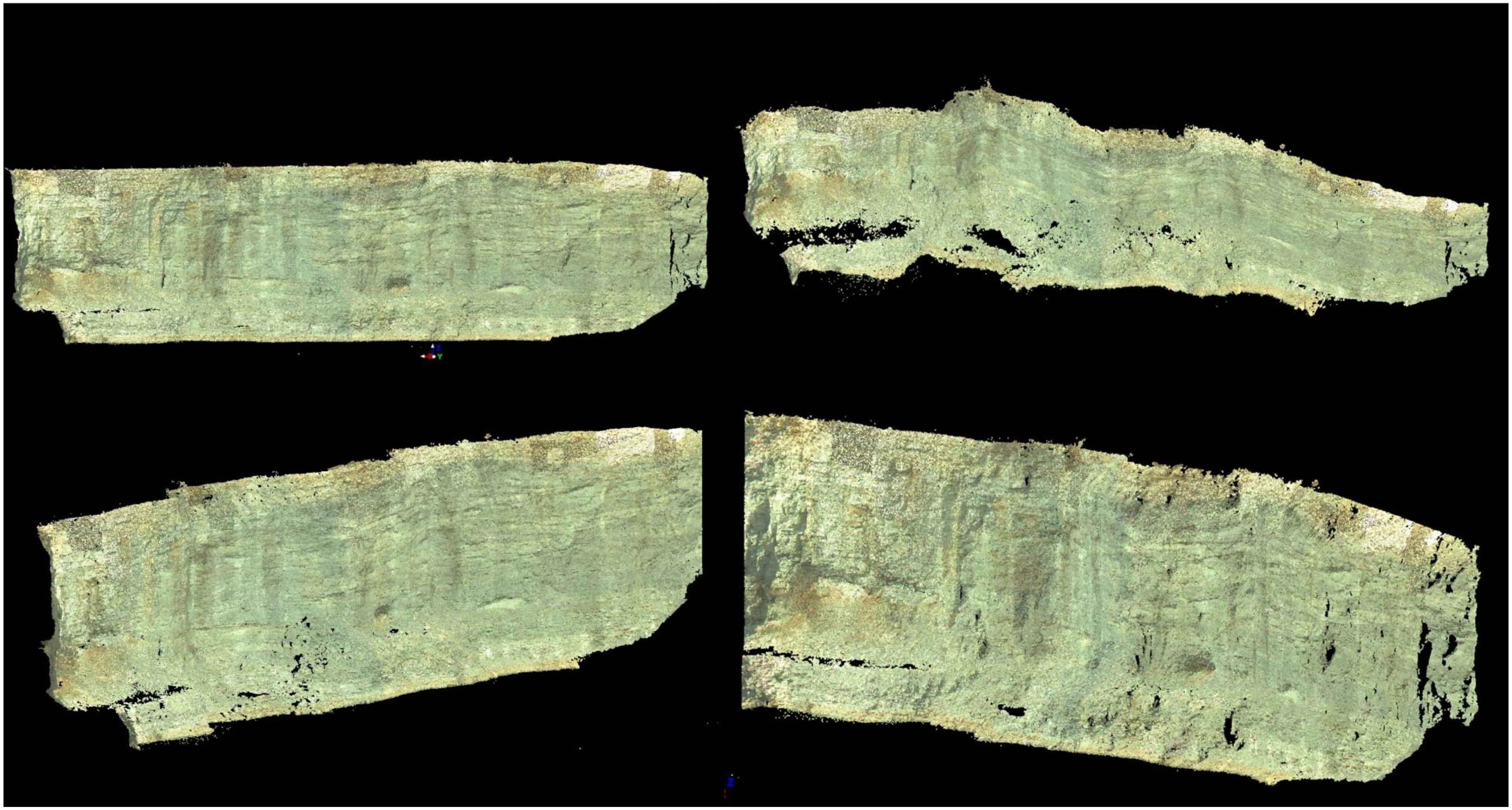

Figure 25. Registration
The registration of multiple scans allows the reduction of data shadows. The above figure is the registration of Location 1 and Location 2.

field. A pseudo well was placed along the LiDAR image to make measurements and produce a stratigraphic column (figure 26; figure27). The assistants of Terrestrial LiDAR allow better interpretation of photographs (figure 28). Figure 29 shows the usefulness of terrestrial LiDAR in the interpretation of geologic features.

Classification through Clustering

Clustering regimes are used in an attempt to classify similar intensities and related to the different lithologies in the field. A classification of raw intensities data shows that the edges of the dataset and angles near perpendicular to the laser scan are classified together (figure 30). Small Subsets of the data showing anastomosing chert were classified using k-means (figure 31). The k-means classification shows that raw intensities can be classified in a schematic to identify a majority of the chert. This method has not been fully optimized for larger datasets. Clustering normalized data shows an improvement in the visualization of the dataset (figure 32).

Figure 26. Orthophoto Terrestrial LiDAR from Cyclone
The exported orthophoto from the terrestrial LiDAR geometrically corrects an image, thus allowing a uniform scales and measurements to be made. The red box highlight the pseudo well measurment

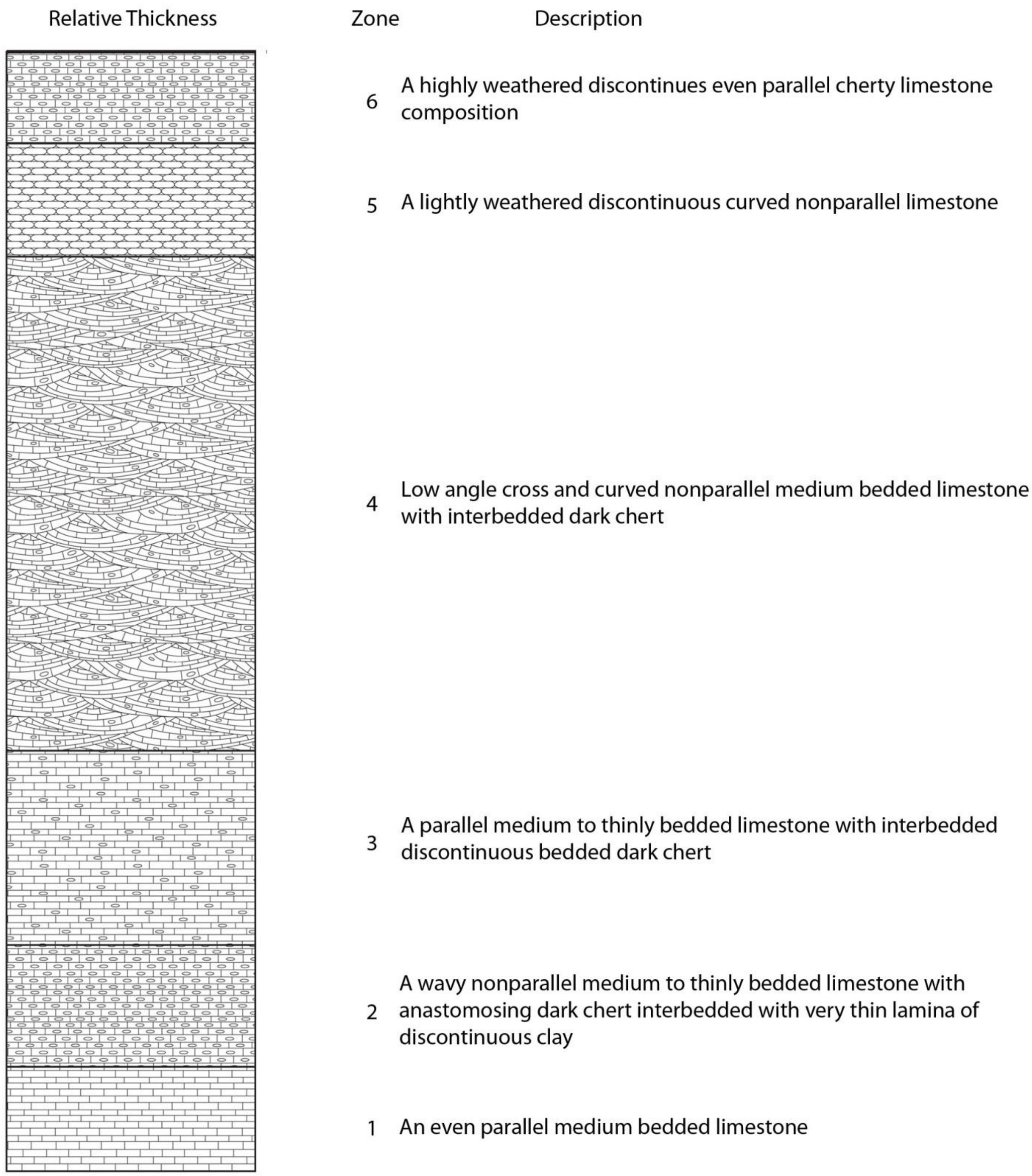

Figure 27. Stratigraphic Column for NW Quarry Wall
The stratigraphic column was created using the assistance of the orthophoto in figure 26. The stratigraphic column uses bedding, lithology, and sedimentary structures in the classification regime.

Figure 28. Photo interpretation
The assistance of LiDAR allowed the improved interpretation of mosaic photos in the research area. The figure outlines different zones, the traces of the different bedding planes, and stratigraphic patterns.

Figure 29. Zonation of the Northwestern Wall
Based on bedding, stratigraphic pattern, and lithology the northwestern face is subdivided into six different sections.

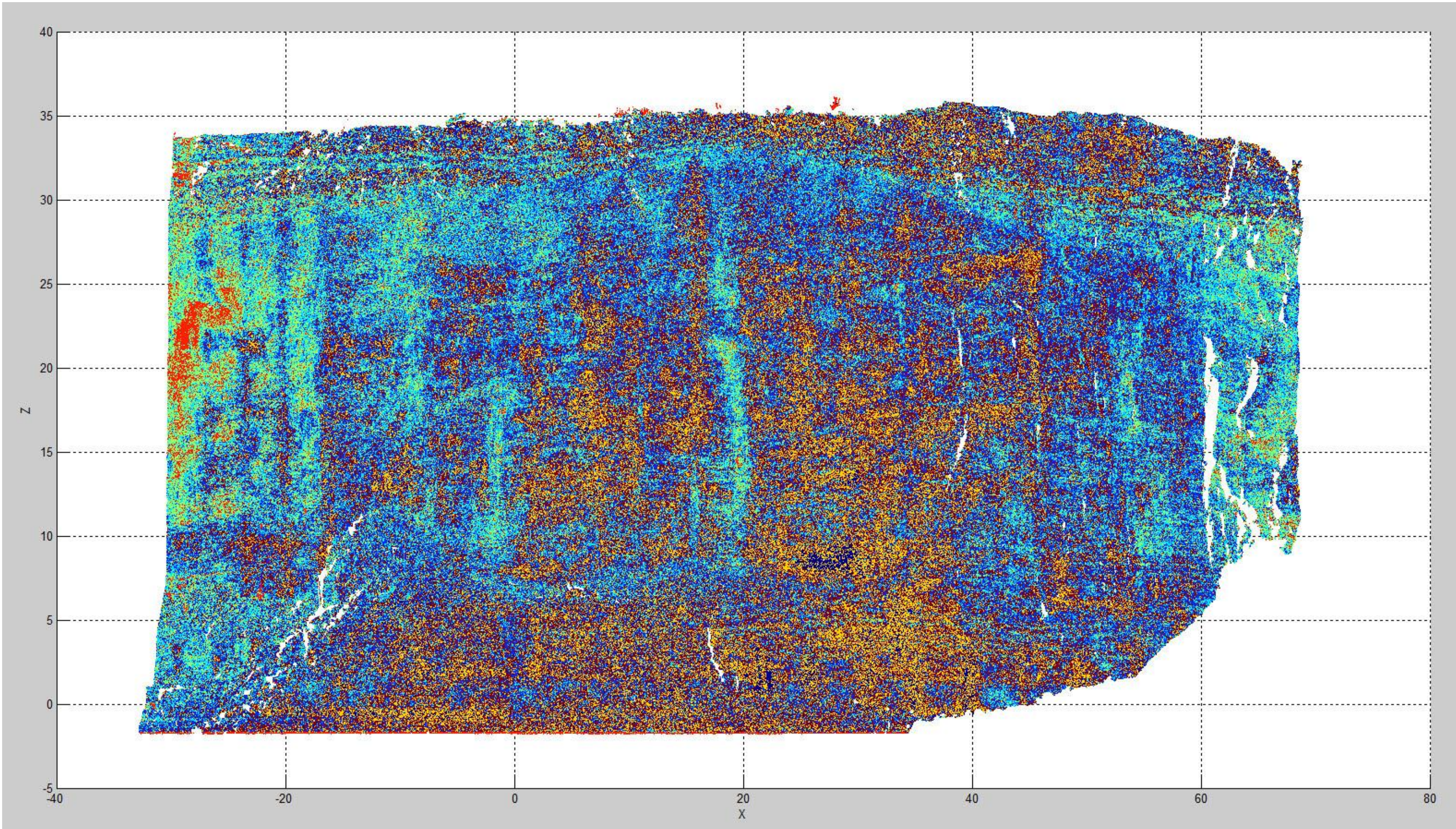

Figure 30. Cluster of Raw Intensity Values
The colors correspond to different cluster intervals. Interpretations of stratigraphic pattern can roughly be made using the raw intensity values. The above figure is classifying intensity values in seven classes. Intensity values show the data is strongly effected by distance because intensities allow map are largely different then surrounding scan. Therefore data must be normalized before full interpretation is possible.

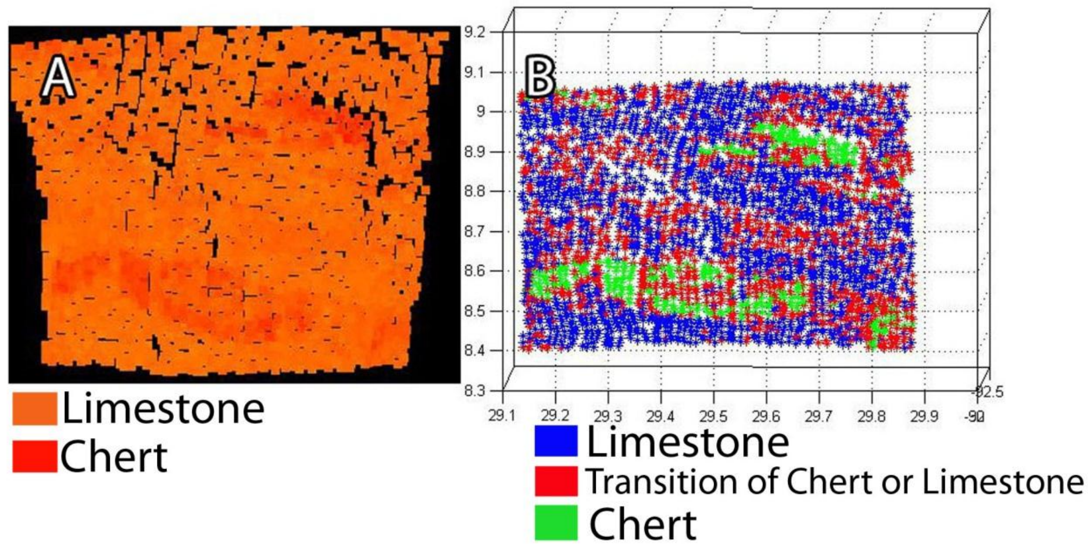

Figure 31. Matlab K-mean classification of Exported TLS Data
The use of k-means on small subset of data shows that chert can be properly interpreted, thus allowing percentages of chert content to be calculated.

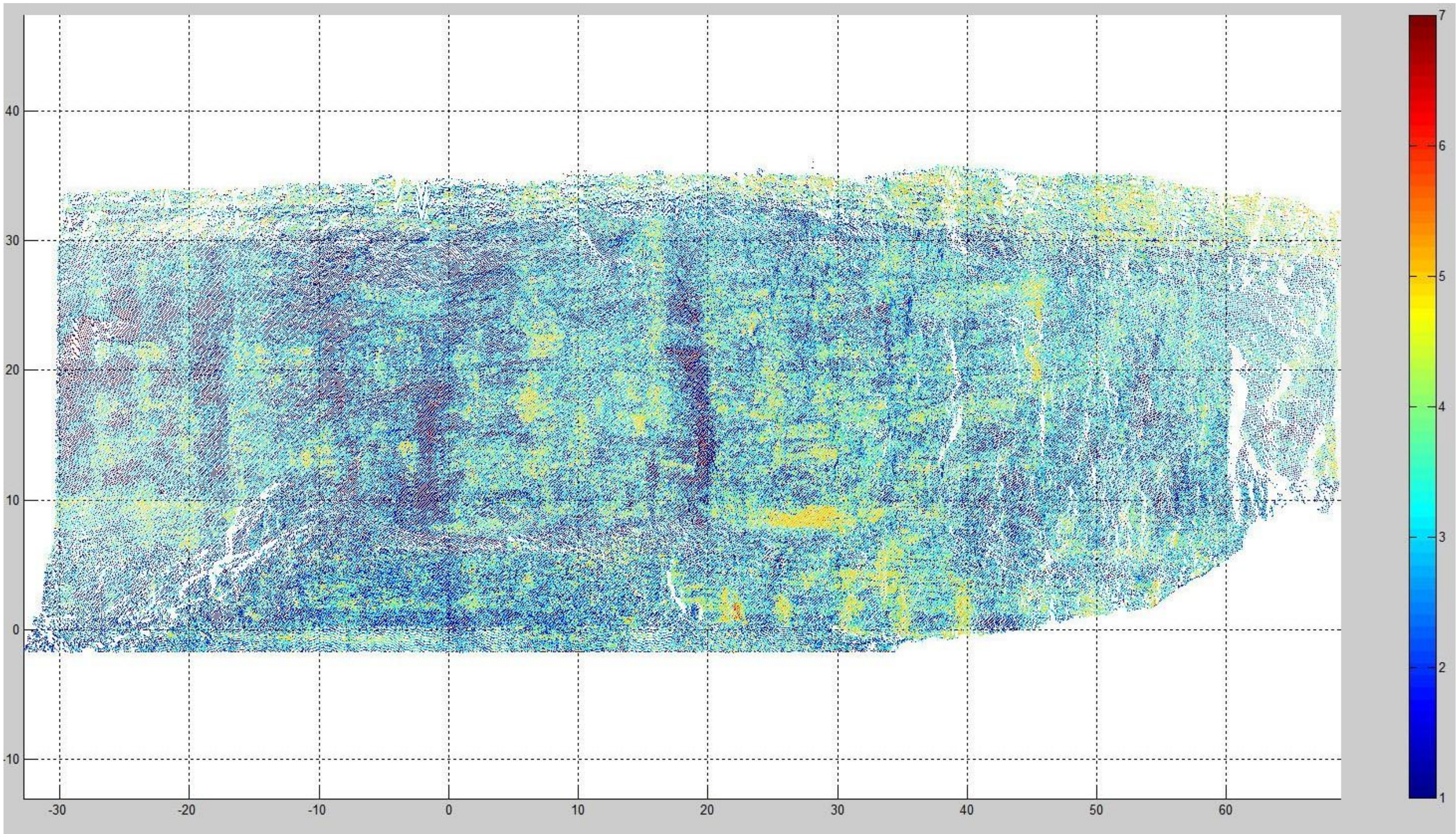

Figure 32. Normalized Intensity Data
The different colors correspond to different cluster class. Normalized data show that stratigraphic pattern and bedding can readily identified. The above figure is classified into 7 classes. The areas cleared through blast or recent weathering show high intensity values and can be strongly made out. Bedding plane and stratigraphic pattern are also clearly seen in normalized data.

Discussion

The unit architecture within the Hindsville Quarry outlines varying transitional periods that give insight into the deposition of the Boone Formation. The sedimentary structures and geometries latterly and horizontally insinuate the varying flow regimes of the Boone Formation. The driving mechanism of flow could be a function of distal turbidities, depositional lobes, the physiographic topography of the region, regional sea level, and/or the depositional setting. The complexities of the sedimentary structures lead to the idea that the structures seen are combination of the above listed mechanism, thus not fitting into an idealized stratigraphic column. These interpretations are a combination of the use of analogues and geologic interpretation.

Analogues

There are comparable formations within the Carboniferous that serve as helpful analogues in explaining the complexities seen in the Hindsville Quarry. Definition and examples of sedimentary structures assist in interpretation. Cross stratification and truncated surfaces are indicative of a significant transport and flow regime (Boggs, 2006). Wilson (1975) describes festoon cross-bed to be formed in moderately strong currents, having lenticular and often truncate lower beds, and is common in outer, seaward parts of shelves. Distal turbidites can form fan shaped wedges and in cross section they can appear as evenly bedded sheets and possibly leading to the deposits of depositional lobes. Depositional lobes features include: development near the mouth of a submarine-fan channels, show absence of basal channeling, usually display thickening upward depositional cycles, and laterally continuous (Shanmugam and Moiola, 1991). According to Gervais and others (2006) “lobes are not entirely sheet-like as previously thought, but are channelized and composed of several units.”

Cherty limestone with concave up truncated surfaces that have wedge shape geometries in the Hare Firod Formation are an example of transported carbonate. These features are interpreted as “onlapping distal lobes of submarine fans, downslope from a local source of turbidity currents” (Davis, 1977). The cherty packstone and grainstone facies of the Tierra Blanca member has large-scale lobate striatal geometries and truncation surfaces. These sedimentary structures are interpreted to be caused by three different possible mechanisms. The transport of carbonates from an isolated up dip point source, the funneling of sand downslope through bathymetric lows, or transport process causing carbonate sand to be focused downslope at specific points (Bachtel and Dorobek, 1998). The Dimple limestone (Atokan) has facies described with cross-beds and are interpreted to be caused by proximal or distal turbidites (Thomsan and Thomasson, 1969). The Ullin formation is composed of grained, bryozoan-crinoidal grainstone with low angle cross-lamination, large scale planar and trough cross-bedding and hummocky cross-stratification. The sediments are believed to be deposited on a storm-dominated ramp (Lasemi et al, 1988).

Geologic Interpretation

The descriptions and interpretations of the segmented zones increase the comprehension and understanding of the Hindsville Quarry.

Zone 1 depicts a transition between St. Joe and Boone Formations (figure 33). A thinning up of this zone, and the pattern of a thin layer of discontinuous chert, two meters of limestone, and then a return of discontinuous chert reinforce this idea.

Zone 2 is an interpretation of wavy bedded rocks represents lobate flow regime (figure 34). Another interpretation of the zone is its resemblance to an idealized distal turbidities stratigraphic column. The presence of pelagic lamination, nodules, and wavy bedded all fit the

Figure 33. Zone 1
Zone 1 shows the bedding thin from medium bedding to thin bedding. The zone appears mostly chert free expt a thin

Figure 34. Zone 2

Zone 2 is a wavy nonparallel medium to thinly bedded limestone with anastomosing dark chert interbedded with very thin lamina of discontinuous clay**.**

description. The contact with the underlying unit is gradual. The chert configuration changes from an anastomosing behavior in zone 2 to a discontinuous bedded pattern in zone 3. Therefore, a possibility of varying flow regime or the delivery mechanism of silica that develops into the penecontemporaneous chert.

Zone 3 is reflective of a return to generally depositional pattern of the Boone Formation (figure 35). The contact between zone 2 and zone 3 is sharp and believed to be another transition in the depositional setting. This zone seems to be pervasive to karst development, with all the caves occurring in this zone around the quarry. A thin section from this zone depicts the energy to be higher and thus possibly on a middle ramp.

The depositional pattern of the isopach of the Boone Formation and the sedimentary structure of Zone 4 of the main wall suggest a lobate depositional style. The sedimentary structures suggest flow to the southeast and reinforce the idea of deposition through lobes (figure 36). The larger scale stratigraphic pattern in zone 4 shows wedge shape geometries crossing and stacking pattern on the main quarry wall (figure 37). Throughout the quarry in the same stratigraphic zone wedge shaped geometries can be identified (figure 38). These features suggest onlapping distal lobes similar to the ones noted in the Hare Firod Formation. Samples from zone 4 show a gradual coursing up and thin sections show a transition from mud-supported to grain-supported texture. According to Shanmugam and Moiola (1985) a coursing up cycle can represent a non-channelized lobe cause by increased sediment delivery. Thin sections suggest the depositional zone occurred higher on the slope and/or closer to source of the transported carbonate. Shelby (1986b) notes the Lower Boone formation appears to be cyclonic at a number of localities and may be caused by turbidity flows or very fine-grained material settling out from the water

Figure 35. Zone 3

Zone 3 is a parallel medium to thinly bedded limestone with interbedded discontinuous bedded dark chert.

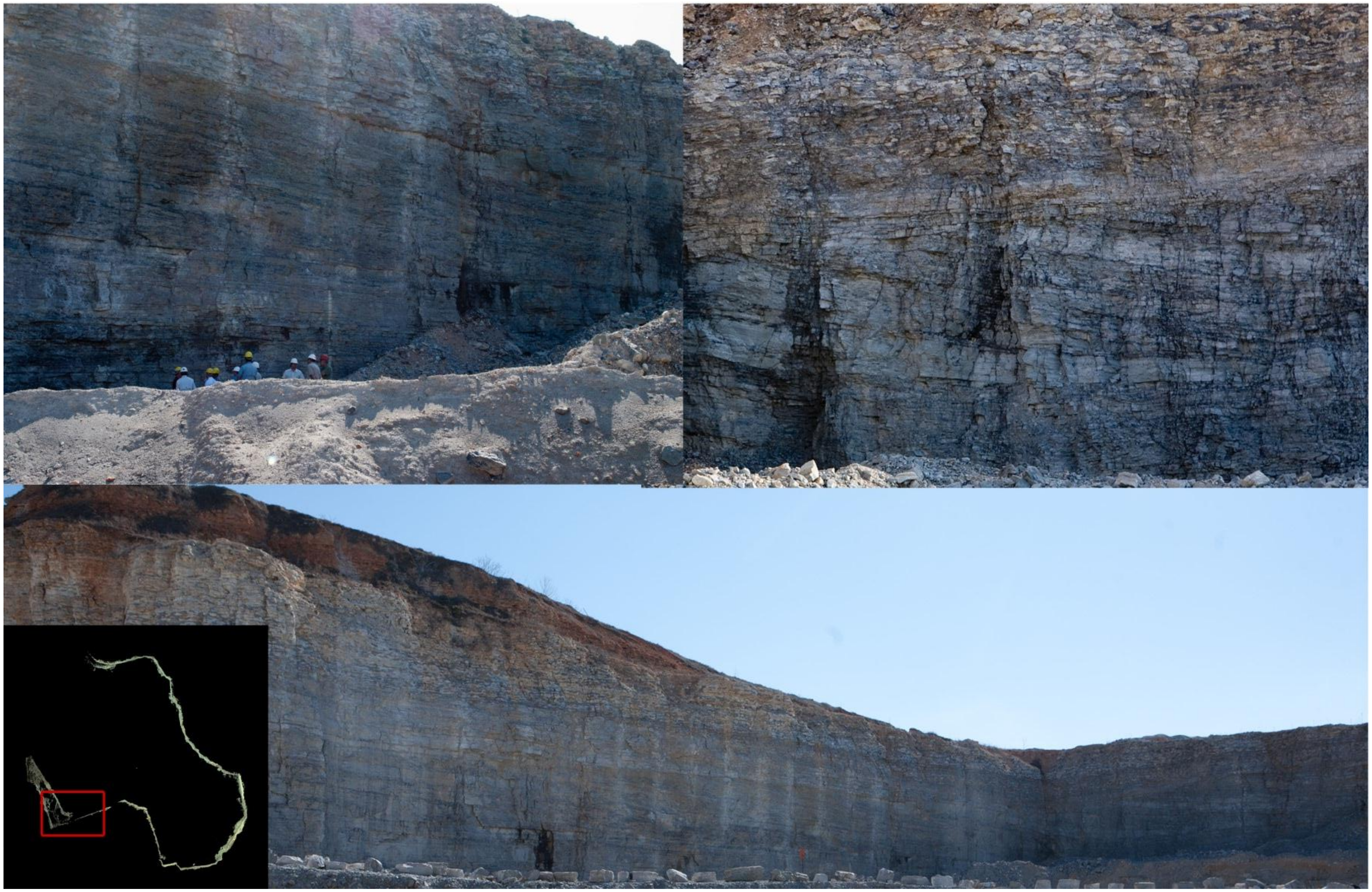

Figure 36. Zone 4

The upper left and upper right photo depict two perpendicular faces of the below faces. The upper left photo shows planes that are generally incline and the upper right shows low angle cross trough beds (this face is trending 60-240 degrees). These beds suggest flow to the south east.

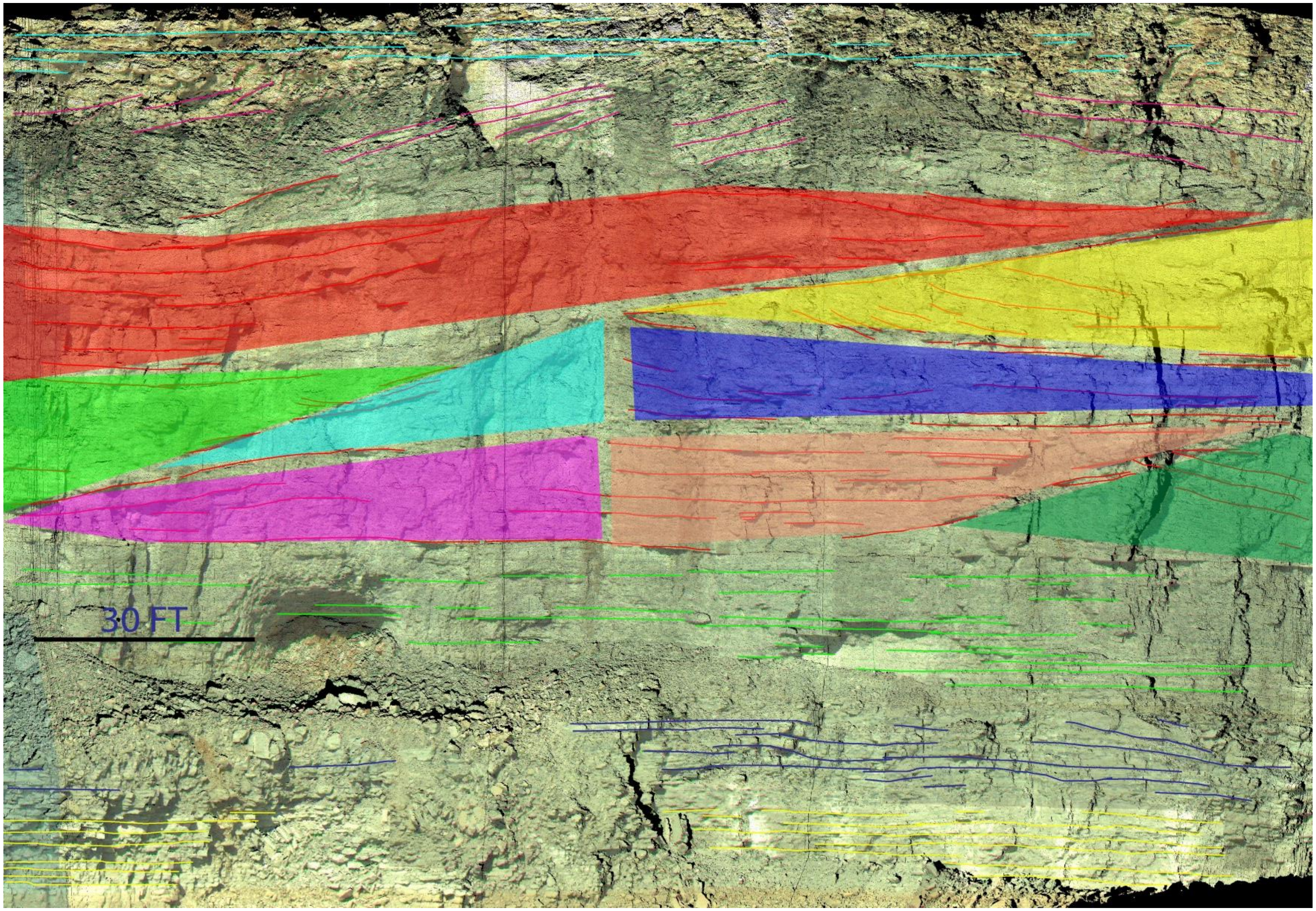

Figure 37. Wedge Shape Geometries in Zone 4
The figure highlights different wedge shape geometries that are present in zone 4. The onlapping of these wedge shape structures are possible onlaps of depositional lobes.

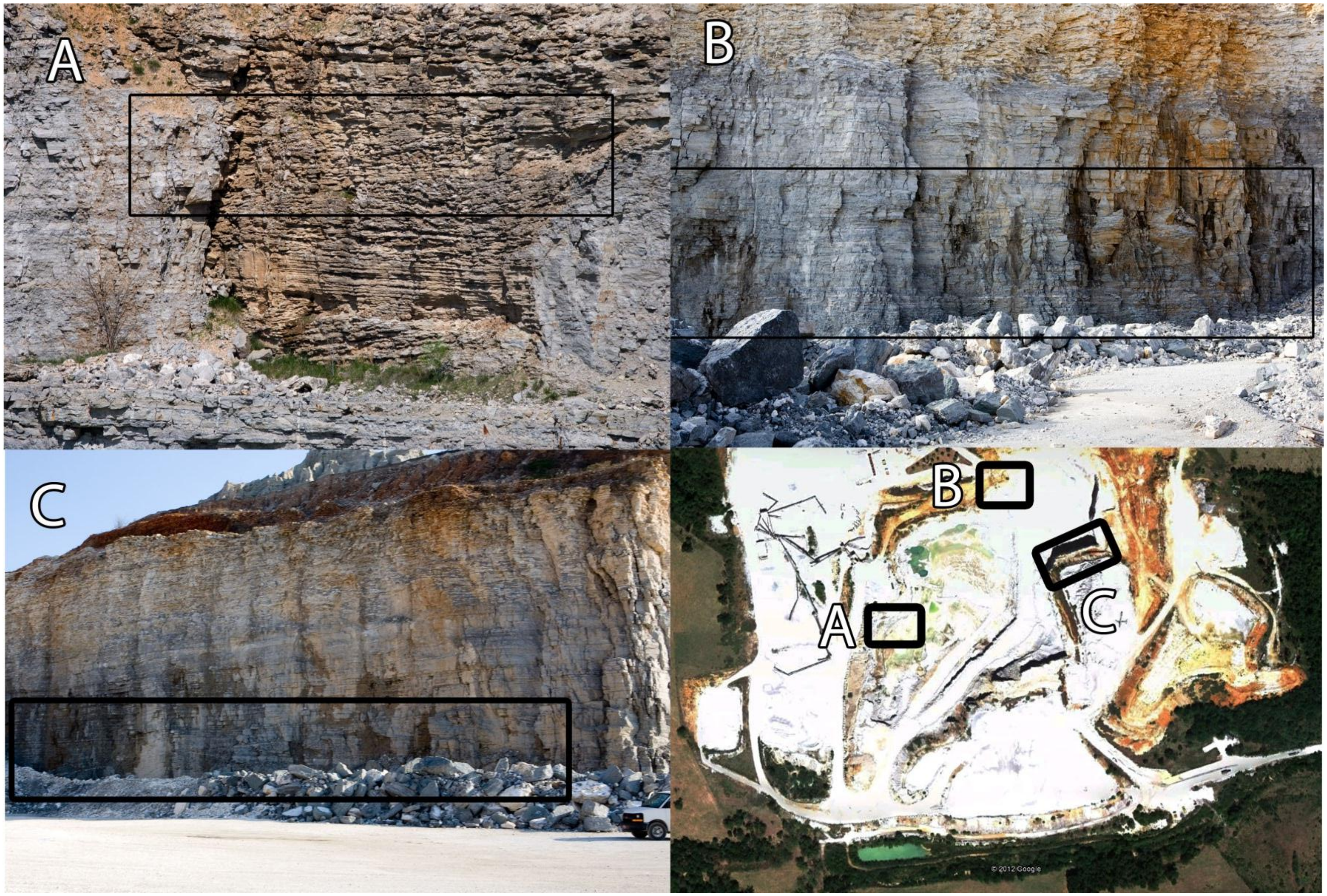

Figure 38. Wedge Shape Geometires in Hindsville Quarry
Localities stratigraphically correlatable to zone four displayed wedge shape geometries. The wedges are highlighted in rectangles in the different images.

column in between periods of active transport. In addition, deposition higher on the ramp allows storm waves to effect sedimentation, thus helping explaining stratigraphic pattern seen in zone 4.

Throughout the quarry zone 5 is depicted as another zone the displays a transition. The contact is sharp and shows a slight color charge. Zone 4 is relatively thinner than other zones and gradually shift into the next zone. This zone is Upper Boone because of its proximity to the resemblance of tripolitic interval developed in the Upper Boone. The transition to the next zone is gradual and could be distinguished identified as tripolitic interval.

The mechanisms of transport of the Boone Formation could occur through turbidity or debris flows, thus can eventually producing a distal fan. The mechanism of the re-sedimentation through turbidity currents can explain the erosional surfaces and wedge shape geometries seen in the Hindsville quarry. Zone 3, 4, and 5 correspond to the B, C, and D Bouma Sequence divisions, but they can be reinterpreted through the creation of bottom current reworking (Shanmugam, 1997). Thin sections show deposition occurred on a ramp, where storm waves could have played a part in the development of the sedimentary structures. The cross bedding in zone 4 is possibly a function of storm waves, ocean currents, or channelized lobes, and are best described as festoon cross-beds. Diffusive process (turbidity currents or debris flows) and physical energy flux (winds, waves, and storms) played a large part in defining the sedimentary structures found within the Hindsville Quarry. These mechanisms demonstrate the use of sub aerial exposures are not needed to explain erosive surfaces.

Terrestrial LiDAR

Terrestrial LiDAR is used to identify stratigraphic pattern, bedding planes, and determine the orientation of inaccessible quarry walls. The effects of distance and incidence angle, resolution of the scan, and the ability to discriminate varying lithologies played a role in the assessment of the geologic outcrops. The intensity values are many investigated and used throughout the study.

The intensity values are used to help register multiple scans and discriminate between lithologies. It is important to reiterate that the Leica C10 scanner uses a wavelength of 530 nm, and water absorption does not play as large a role as with the Z+F scanner, which is at 1530 nm. Relatively the chert appeared to reflect less light back to the scanner, thus having lower intensity values, and being able to identify the chert in Cyclone. The effect of distance and incidence angle decreases the values of intensity as well (Figure13; Figure39). The possibility of limestone having a lower intensity because of incidence angle is an issue. This can be seen at a vertical interval on the main quarry face, which could have been a blast location. Surfaces that have been recently cleared due to erosion show intensity values that appear to be higher (Figure 39). The identification of lithology and stratigraphic pattern can be seen in cyclone. Although a numerical value of intensity has not been established to discriminate chert from limestone and the intricacies of incidence angle could be playing a role. The intensity color map in cyclone allowed stratigraphic pattern to be identified in zone 4. The intensity color map assisted greatly in flowing and identifying truncated surfaces in the zone 4. The use of other varying visualization techniques in Cyclone also assisted in the assessment of the geologic outcrop.

Each of the scans at the Hindsville quarry was taken at 1 cm resolution. For this locality the resolution was sufficient to see and trace stratigraphic pattern and bedding planes. Most of

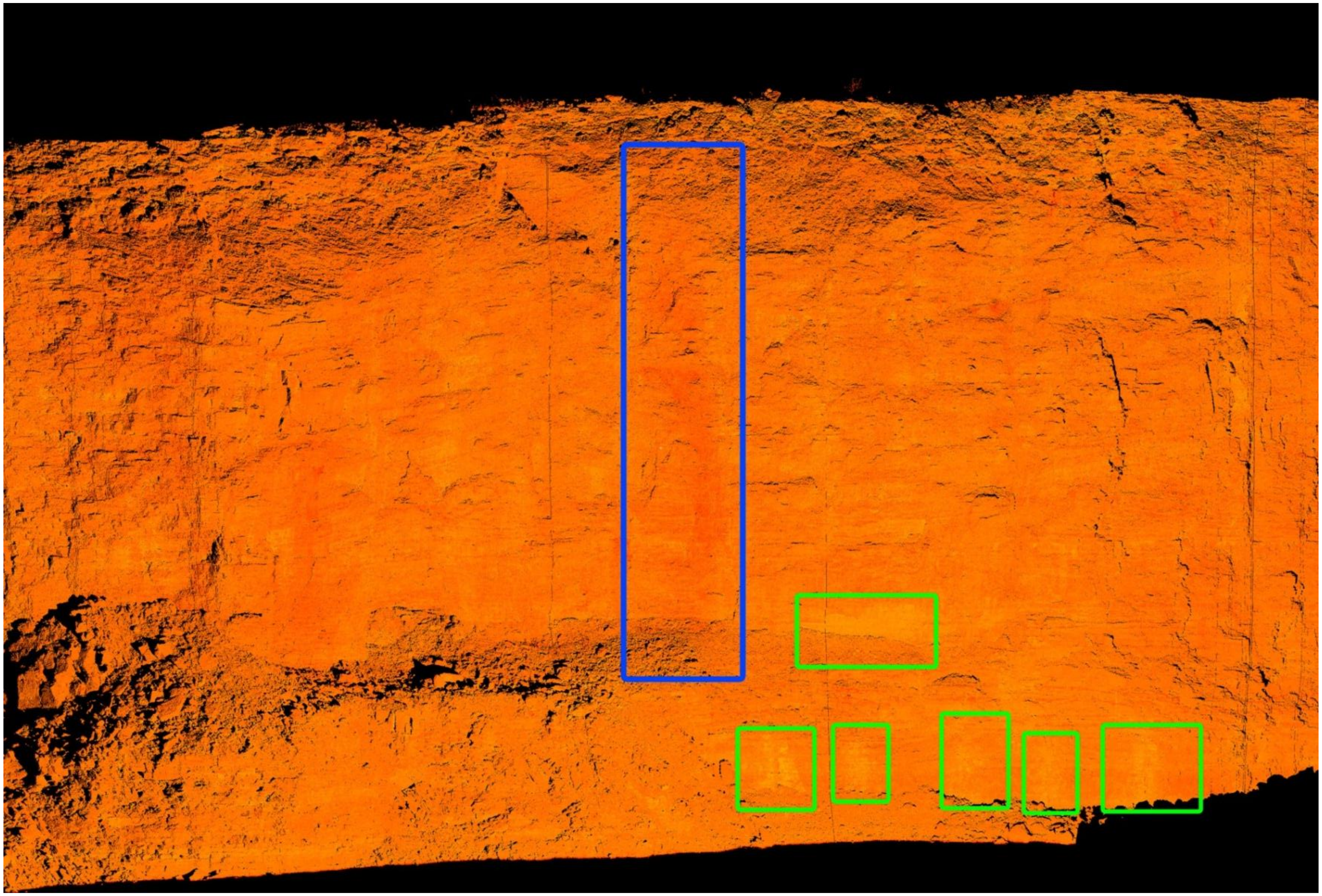

Figure 39. Intensity Evaluation
The different boxes are where intensity has been effected by incidence angel or erosion. The blue box highlights an area where the incidence angel may have played a role in the decrease of intensity. The green boxes highlight different areas showing erosion and there higher intensity value returns.

the interpretation and measurements were taken from scan 1. The registered scan did provide some insight, but the individual scan did work adequately. The photo texture overlay assisted with large scale stratigraphic pattern and bedding planes but was not a lot of help for the assistance of intricate detail. The texture overlay resembled the outcrop, thus allowing orienting oneself from the field. This visualization capability is a great transition from field to computer station.

The surveyed dataset allowed detail measurement to be accomplished. The use of the measurement capabilities with the LiDAR allowed the understanding of thickness of beds, height of quarry wall, and size of the sedimentary structures. Without the assistance of terrestrial LiDAR the field, measurements would not be accessible nor as accurate.

Scan data imported into Cyclone attempted to discriminate lithology using classification algorithm k-means. After distance normalization, stratigraphic boundaries can be identified, especially the transition of zone 4 to zone 5, as well as other boundaries, but cannot be seen as consistently in Cyclone. Another distinguishing feature in the clustering is the fresh surfaces. The intercalated nature of the quarry wall makes it difficult for visually being able to constantly distinguish chert from limestone. The size of the data set makes it hard to navigate and directly compare the entire quarry wall. A subset of the dataset showed the clustering into 3 classes can mimic the chert pattern, thus allowing quantitative estimations of chert values. This method has not been optimized for a larger dataset, but shows the possibility of the data collected. The clustering works in a manner by grouping values of similar intensity around a centroid. But the values will change in another section due to distance and incidence angle. Therefore, a standard set of intensity values is not assigned to identify chert or limestone.

The non-contact techniques of investigating geologic outcrops through Terrestrial LiDAR cannot replace transitional methods of geologic investigation. These remote sensing techniques assist in the quantitative and qualitative descriptions and information obtained from the geologic outcrop. The limited access and accessibility of location greatly improved in the stratigraphic pattern interpretation. The photography from the site did not adequately portray geologic features as well as the Terrestrial LiDAR. In the quarry chert was not always readily identifiable, but within the LiDAR scan the intensity color map greatly assisted in the identification. The scan showed where to look, thus helping define lithology pattern better. The scan in Cyclone depicted an adequate resemblance of the quarry and allowed the time need to investigate and define the stratigraphic features of the geologic outcrop.

Conclusion

The Hindsville Quarry is present to numerous transitional zones that give insight into the deposition of the Boone Formation. The sedimentary structures within the quarry are reflective of diffusive process (turbidity currents or debris flows) and physical energy flux (winds, waves, and storms). These driving mechanisms produced distal turbidities and depositional lobes. The complexities of the Boone formation within the Hindsville quarry are not easily defined, and the sedimentary structures are combination of the numerous mechanism. The erosional surfaces and distinctive bedding surfaces can be explained through diffusive process and physical energy flux, thus explanation through sub aerial exposures is not necessary.

Terrestrial LiDAR assisted in the limited time access and inaccessible portion of the outcrop at the Hindsville quarry. The quarry is operated by APAC and permission is needed to access the quarry, as well as a chaperone is need while doing fieldwork. The quarry wall can reach up to 100 feet high and a hands on investigation is inaccessible at these heights. Thus Terrestrial LiDAR played a major role in helping identify stratigraphic pattern at the Hindsville Quarry. The 1 cm resolution and head on scan from location 1 served as enough bases for basic interpretation of stratigraphic pattern and bedding plane. The development of stratigraphic columns was created through measurements of bedding planes and sedimentary structures. This is capable because of the resolution provided through terrestrial LiDAR. The classification and numerical discrimination of chert and limestone is more difficult. Although, the visually generalization can be made.

References

Bachtel, Steven L. and Borobek Steven L., 1998, Mississippian Carbonate Ramp-To Basin Transistions in South-Central New Mexico: Sequence Stratigraphic Response to Progressively Steepening Outer Ramp Profiles, Journal of Sedimentary Research, v 68, no 6, p 1189-1200

Ball, M.M., 1967, Carbonate Sand Bodies of Florida and the Bahamas, Journal of Sedimentary Petrology, vol 37, no 2, p 556-591

Bellian, J.A., Kerans, C, Jennette, D.C., 2005, Digital Outcrop Models: Applications of Terrestrial Scanning LiDAR Technology in Stratigraphic Modeling, v 75, no 2, p 166-176

Bogg Jr, Sam, 2006, Principles of Sedimentology and Stratigraphy 4th Edition, Pearson –Prentice Hall, Upper Saddle River, New Jersey, p 662

Burchette, T.P., and Wright, V.P., 1992, Carbonate ramp depositional systems, Sedimentary Geology, v 79, p 3-57

Burton, Darrin, Dulap, Dunlap, Dallas B., Wood, Lesli J., and Flaig, Peter P., 2011, LiDAR Intensity as A Remote Senosor of Rock Properties, Journal of Sedimentary Research, v. 81, p 339-347

Chinn, Alvin A and Konig, Ronald H, 1973, Stress Inferred from Calcite Twin Lamellae in Relation to Regional Structure of Northwest Arkansas, Geological Society of America Bulletin, v 84, p 3731-3736

Davis, Clayton Yari, 2007, Structural, Stratigraphic, and Reservoir Characteristics of Natural Gas Production from the Boone Formation, Batson and Ozone Fields, Arkoma Basin, Western Arkansas, Unpublished Master's Thesis

Davies, Graham R., 1977, Turbidites, Debris Sheets, and Truncation Structures in Upper Paleozoic Deep-Water Carbonates of the Sverdrup Basin, Arctic Archipelago, SEPM Special Publication, no 25, p 221-247

Dorrik, A.V. Stow, David, G. Howell, and C. Hans Nelson, 1985, Sedimentary, Tectonic, and Sea-Level Control, Submarine fans and related turbidite systems, Spring-Verlag, New York, p 15-22

Fabuel-Perez, I., Hodgetts, D., Redfern, J., 2010, Integration of digital outcrop models (DOMs) and high resolution sedimentology – workflow and implications for geological modeling: Oukaimeden Sandstone Formation, High Atlas (Morocco), Petroleum Geoscience, v 16, p 133-154

Francheschi, M., Teza, G., Preto, N., Pesci, A., Galgaro, A., and Girardi, S., 2009, Discrimination between marls and limestones using intensity data from terrestrial laser scanner: Journal of Photogrammetry and Remote Sensing, v. 64, p 522-528

Gervais, Anne, Savoye, Bruno, Mulder, Thierry, and Gonthier, Eliane, 2006, Sandy modern turbidite lobes: A new insight from high resolution seismic data, Marine and Petroleum Geology, v 23, p 485-502

Giles, A.W., 1935, Boone Chert: Geological Society America Bulletin, v 46, no 12, p 1814-1867

Graham, Stephan A., Dickinson William R., and Ingersoll Raymon V., 1975, Himalayan-Bengal Model for Flysch Dispersal in the Appalachian-Ouachita System, Geological Society of America Bulletin, v 86, p 273-286

Gutschick, Raymond C., and Sandberg, Charles A., 1983, Mississippian Continental Margins of the Conterminous United States, SEPM Special Publication, v 33 no 6, p 79-96

Hudson, Mark R., 2000, Coordinated strike-slip and normal faulting in the southern Ozark dome of northern Arkansas: Deformation in a late Paleozoic foreland, Geology, v 28, p 511-514

Handford, Robertson C. and Loucks, Robert G., 1993, Carbonate Depositional Sequences and Systems Tracts—Responses of Carbonate Platforms to Relative Sea-Level Changes, AAPG Memoir 57, p 3-38

Hudson, Mark R., 2001, Coordinated strike-slip and normal faulting in the southern Ozark dome of northern Arkansas: Deformation in a late Paleozoic foreland, Geology, v 28, issue 6, page 511-514

Kaasalainen, Sanna, Jaakkola Anttoni, Kaasalainen Mikko, Krooks Anssi, and Kukko, Antero, 2011, Analysis of Incidence Angle and Distance Effects on Terrestrial Laser Scanner Intensity: Search for Correction Methods, Remote Sens., v 3, no 10, p 2207-2221

Lane, H. Richard, 1978, The Burlington Shelf (Mississippian, North-central United States), Geologica et palaeontonlogica, v 12, p 165-176

Lane, Richard H., and De Keyser, T. L.,1980, Paleogeography of the Late Early Mississippian (Tournaisian 3) in the Central and Southwestern United States, *in* Fouch, T.D., and Magathan, E.R., eds., Paleozoic paleogeography of the west-central United States: Society of Economic Paleontologists and Mineralogists, Rocky Mountain Section, Paleogeography Symposium 1, p. 149-162

Lasemi, Zakaria, Norby, Rodney D., Treworgy, Janis D., 1998, Depositional facies and sequence Stratigraphy of Lower Carboniferous bryozoan-crinoidal carbonate ramp in the Illinois Basin, mid-continent USA, Geological Society, London, Special Publication 1998, v 149 , p 369-395

Lillie, Robert J, Nelson, K. Douglas, Voogd, Beatrice De, Brewer, Jonathan A., Oliver, Jack E., Brown, Larry D., Kaufman, Sidney, and Viele, George W., 1983, The American Association of Petroleum Geologists Bulletin, v 67, no 6, p 907-931

Liner, Jeff,1980, Lithostratigraphy of The Boone Limestone (Lower Mississippian) northwest Arkansas, Unpublished Master's Thesis, University of Arkansas, p 88

Manger, WL, 2012, An Introduction to the Lower Mississippian (Kinderhookian-Osagean) Geology of the Tri-State Region, Southern Ozarks, Guide Book: Vitruvian Exploration LCC, p 60

Manger, WL, Shelby PR, and Farris, SG, 1988, Devonian-Lower Mississippian Lithostratigraphy, Northwestern Arkansas, v 65, issue 4, p 223-231

Manger, WL, and Shelby, PR, 2000, Natural-Gas Production from the Boone Formation (Lower Mississippian), Northwestern Arkansas, Oklahoma Geological Survey Circular, v 101, p 163-169

Mazzullo, S., Boardman, D.R., and Wilhite, B., 2011, Lithostratigraphic Architecture of the Mississippian Reeds Spring Formation (Middle Osagean) in Southwest Missouri, Northwest Arkansas, and Northeast Oklahoma: Outcrop Analog of Subsurface Petroleum Reservoirs, in Shale Shaker: The Journal of the Oklahoma City Geological Society, Vol. 61, March/April 2011, No. 5, p 254-269

Olariu, M.I., Aiken, C.L.V., Xu, X., 2011, Interpretation of channelized architecture using three-demensional photo real models, Pennsylvanian deep-water deposits at Big Rock Quarry, Arkansas, Marine and Petroleum Geology, v 28, p 1157-1170

Olariu, Mariana I., Ferguson, John F., Aiken, Carlos L.V.,Xu, Xucming, 2008, Outcrop fracture characterization using terrestrial laser scanner: Deep-water Jackfork sandstone at Big Rock Quarry, Arkansas, Geosphere, v 4, no 1, p 247-259

Pfeifer N, Dorninger P, Haring A, and Fan H, 2007, Investigating Terrestrial Laser Scanning Intensity Data: Quality and Functional Relations, Proceedings International Conference on Optical, p 328-337

Shanmugam, G, 1997, The Bouma Sequence and the turbidite mind set, Earth-Science Reviews 42, p 201-229

Shanmugam, G and Moiola RJ, 1985, Submarien Fan Models: Problems and Solutions, Submarine fans and related turbidite systems, Spring-Verlag, New York, p 29-34

Shanmugam, G and Moiola RJ, 1991, Types of Submarine Fan Lobes: Models and Implications, The American Association of Petroleum Geologist Bulletin, v 75, no 1, p 156-179

Shelby, Phillip R, 1986a, Depositional History of the St. Joe and Boone Formation in Northern Arkansas, Proceedings Arkansas Academy of Science, V 40, p 66-71

Shelby, Phillip R, 1986b, Depositional History of the St. Joe and Boone Formation in Northern Arkansas, M.S. thesis, University of Arkansas, p 92

Stanton, Gregory P. 1993. Processes and controls affecting anisotropic flow in the Boone-St. Joe quifer in northwestern Arkansas: unpublished M.S. thesis, University of Arkansas.

Thomson, Alan F. and Thomasson Ray M., 1969, Shallow to Deep Water Facies Development in the Dimple Limestone (Lower Pennsylvanian) Marathon Region, Texas, Society Economic Paleontologists Mineralogists Special Publication, v 14, p 57-78

Van Den Heuvel, Peter, 1979, Petrography of the Boone Formation, Northwest Arkansas, Unpublished Master's Thesis, p 75

Wilson, C.E., Aydin, A., Karimi-Fard, M., Durlofsky, L.J., Sagy, A., Brodsky, E.E., Kreylos, O., and Kellogg, L.H., 2011 , From outcrop to flow simulation: Constructing discrete fracture models from a LiDAR survey, AAPG Bulleting, v 95, no 11, p 1883-1905

Wilson, James Lee, 1975, Carbonate Facies in Geologic History, Springer-Verlag, New York, p 471

Appendix A: Normalization A

Appendix A includes Matlab algorithms that normalizing the data set

```
a=load('comp1.txt',' ');

r = sqrt(a(:,1).^2 + a(:,2).^2 + a(:,3).^2);
I=mean(a(:,4));
p=polyfit(r,I,2);
y=polyval(p,r);
res=y-I;
mxi=max(res);
mni=min(res);
T=[mni,1;mxi,1;];
B=[0;255];
A=T\B;
yn=A(1)*res+A(2);
scatter(r,yn)
xlabel('distance'),ylabel('Normalized Intensities')
```

After the algorithm is applied normalized data in figure 14 is acquired. The algorithm showed to normalized data with respect to incidence angle.

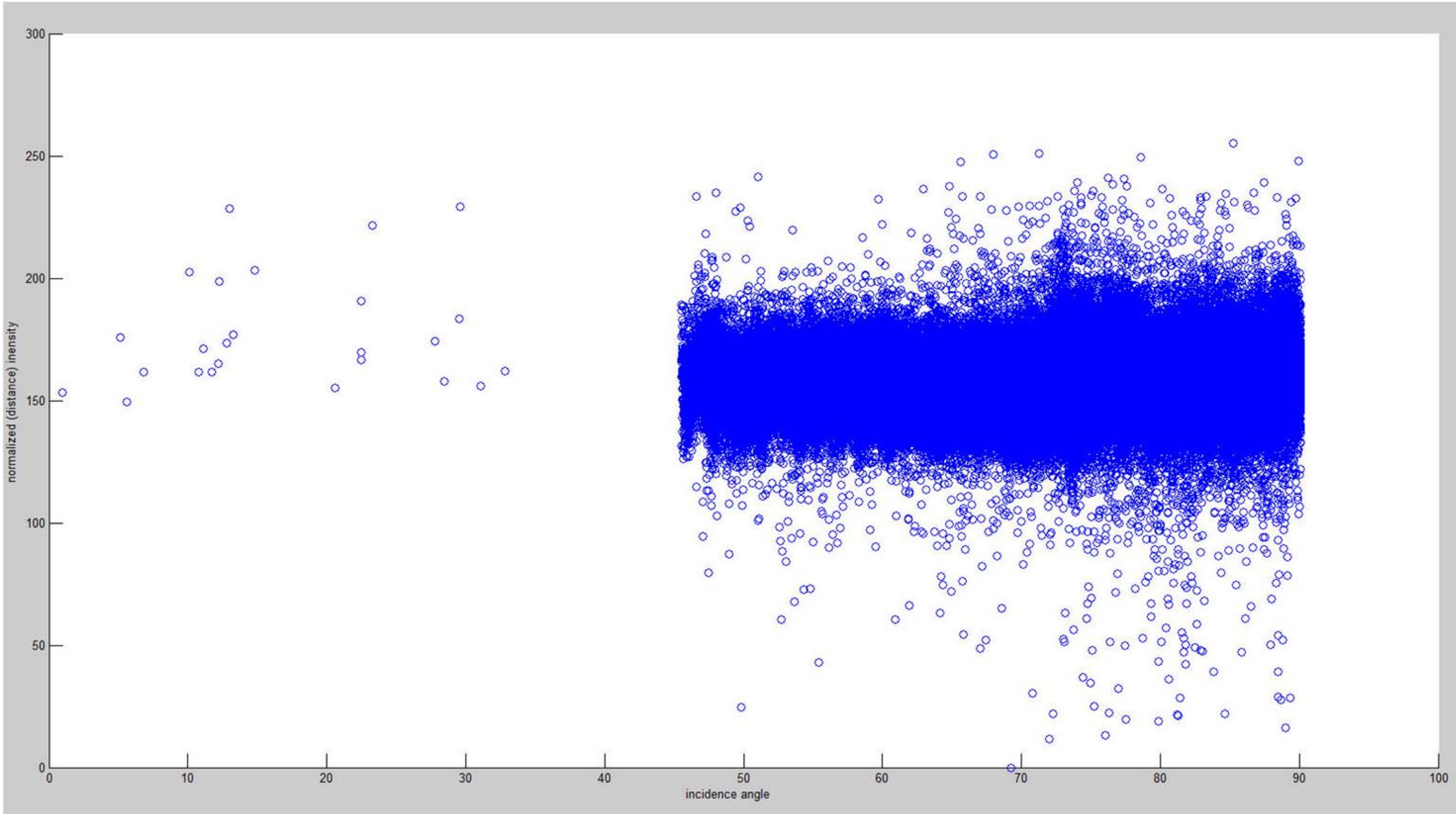

Figure A1: Incidence Angle Normalized
The Matlab algorithm listed in A1 allowed the normalization of incidence angle.

Appendix B: Clustering in Matlab

Appendix B contains the algorithm used to cluster and create figures 31. Multiple subsets were run using this algorithm

Matlab m-file

```
% Step to cluster and graph LiDAR Data
%-----------------------------------------------------------

clear all

a=load('sz2_2.txt',' ');

% Convert from Cartesian to Spherical to get the scanner to point
% distance(r)

[azimuth,elevation,r]=cart2sph(a(:,1),a(:,2),a(:,3));
jj=[a(:,1),a(:,2),a(:,3),a(:,4)];

%Normalize the data by Identisity / radius
ni=a(:,4)./r;

%Classify and Cluster into three groups
ID=kmeans(jj,3);

%split up matrix for easier referenceing

x=a(:,1);y=a(:,2);z=a(:,3);

%graph
figure(1)
hold on, box on, grid on
scatter3(x(ID==1),y(ID==1),z(ID==1),'r*')
scatter3(x(ID==2),y(ID==2),z(ID==2),'g*')
scatter3(x(ID==3),y(ID==3),z(ID==3),'b*')
%scatter3(x(ID==4),y(ID==4),z(ID==4),'b*')
campos([-22,-44,18])
hold off

figure(2)
hist(ni)

disp('class 1 red')
disp('class 2 green')
disp('class 3 blue')

%Calculating percentage
find1=find(ID==1);find2=find(ID==2);find3=find(ID==3);
```

```
p1=size(find1)/size(ID)*100;p2=size(find2)/size(ID)*100;p3=size(find3)/size(I
D)*100;
value1=ni(find1);value2=ni(find2);value3=ni(find3);
mx1=max(value1); mn1=min(value1);rn1=range(value1);
mx2=max(value2); mn2=min(value2);rn2=range(value2);
mx3=max(value3); mn3=min(value3);rn3=range(value3);
vall=[1 mx1 mn1 rn1 p1;2 mx2 mn2 rn2 p2;3 mx3 mn3 rn3 p3];

disp('     Class      Max       Min      Range      %')
disp(vall);

%percentage with lowerst ni values are assumed to be chert based on
%geomotry
```

Table B1. Results from using cluster algorithm

File	Class	max	min	range	%
sz1	1	-16.4827	-17.9065	1.423795	31.38565
	2	-15.9234	-16.4826	0.559231	45.65099
	3	5.31677	-15.9233	21.24012	22.96337
sz1_2	1	-10.0418	-16.3779	6.33612	20.48518
	2	-16.3781	-16.9614	0.583369	48.48205
	3	-16.9617	-18.7081	1.746434	31.03277
sz2	1	-8.25986	-15.6987	7.438814	31.01431
	2	-15.6987	-16.3888	0.690114	50.83788
	3	-16.3888	-19.8055	3.416648	18.14781
sz2_2	1	-13.9631	-14.7495	0.786387	36.82346
	2	-14.7524	-17.0296	2.277174	9.92269
	3	-12.8062	-13.9625	1.156218	53.25387
sz3	1	-15.5851	-16.2262	0.641056	47.43523
	2	-16.2263	-18.5178	2.291511	24.94935
	3	-13.444	-15.5851	2.141069	27.61542
sz4	1	-15.6937	-16.3294	0.635744	51.2263
	2	-11.3	-15.6936	4.393639	28.5388
	3	-16.3295	-20.9634	4.633992	20.2349
	Low	**High**			
chert avg	-16.1902	-18.8218			